Bioorganic Chemistry 83 (2019) 595–610

Contents lists available at ScienceDirect

Bioorganic Chemistry

journal homepage: www.elsevier.com/locate/bioorg

Syntheses, *in vitro* urease inhibitory activities of urea and thiourea derivatives of tryptamine, their molecular docking and cytotoxic studies

Kanwal[a], Majid Khan[a], Arshia[a], Khalid Mohammed Khan[a,e,*], Shahnaz Parveen[d], Muniza Shaikh[b], Narjis Fatima[a], M. Iqbal Choudhary[a,b,c,*]

[a] H. E. J. Research Institute of Chemistry, International Center for Chemical and Biological Sciences, University of Karachi, Karachi 75270, Pakistan
[b] Dr. Panjwani Centre for Molecular Medicine and Drug Research, International Center for Chemical and Biological Sciences, University of Karachi, Karachi 75270, Pakistan
[c] Department of Biochemistry, Faculty of Sciences, King Abdulaziz University, Jeddah 21412, Saudi Arabia
[d] PCSIR Laboratories Complex, Karachi, Shahra-e-Dr. Salimuzzaman Siddiqui, Karachi 75280, Pakistan
[e] Department of Clinical Pharmacy, Institute for Research and Medical Consultations (IRMC), Imam Abdulrahman Bin Faisal University, P.O. Box 1982, Dammam 31441, Saudi Arabia

ARTICLE INFO

Keywords:
Tryptamine derivatives
Structure-activity relationship
Urease inhibitory activity
Gastric ulcers
Urolithiasis
Docking studies
Cytotoxicity

ABSTRACT

Urease is an enzyme of amidohydrolase family and is responsible for the different pathological conditions in the human body including peptic ulcers, catheter encrustation, kidney stone formation, hepatic coma, encephalopathy, and many others. Therefore, the search for potent urease inhibitors has attracted major scientific attention in recent years. Urea and thiourea derivatives of tryptamine (**1–25**) were synthesized *via* reaction of tryptamine with different substituted phenyl isocyanates/isothiocyanates. The synthetic compounds were evaluated for their urease enzyme inhibitory activity and they exhibited good inhibitory potential against urease enzyme in the range of (IC_{50} = 11.4 ± 0.4–24.2 ± 1.5 μM) as compared to the standard thiourea (IC_{50} = 21.2 ± 1.3 μM). Out of twenty-five compounds, fourteen were found to be more active than the standard. Limited structure-activity relationship suggested that the compounds with CH_3, and OCH_3 substituents at aryl part were the most potent derivatives. Compound **14** (IC_{50} = 11.4 ± 0.4 μM) with a methyl substituent at *ortho* position was found to be the most active member of the series. Whereas, among halogen substituted derivatives, *para* substituted chloro compound **16** (IC_{50} = 13.7 ± 0.9 μM) showed good urease inhibitory activity. These synthetic derivatives were found to be non-cytotoxic in cellular assay. Kinetic studies revealed that the compounds **11**, **12**, **14**, **17**, **21**, **22**, and **24** showed a non-competitive type of inhibition. *In silico* study identified the possible bindings interactions of potential inhibitors with the active site of enzyme. These newly identified inhibitors of urease enzyme can serve as leads for further research and development.

1. Introduction

Urease, an enzyme of family amidohydrolases, catalyzes the hydrolysis of the amide bonds of urea into carbon dioxide and ammonia. It has been isolated from various sources, including plants, bacteria, and fungi. It was the first enzyme to be crystallized [1], containing two nickel atoms bridged through hydroxide ion and oxygen atoms of lysine carbamate residue [2–4]. The catalytic action of urease results in an increase in pH with important consequences in biomedical and agricultural fields [5,6]. The over-expression of urease contributes in diseases, such as tuberculosis [7], yersiniosis, [8] and cryptococcosis [9]. Urease is also responsible for different types of gastrointestinal, as well as urinary tract infections, including catheter encrustation, kidney stone formation, hepatic coma, encephalopathy, and pyelonephritis [10]. Bacterial urease over-expression is also accountable for peptic ulcers and urolithiasis which may be due to the *Helicobacter pylori* and *Proteus mirabilis*, respectively. Similarly in agriculture, over-expression of soil bacterial urease contributes to the over-production of ammonia by degradation of urea fertilizer [11], thus leading to environmental and economic problems [12]. Therefore, the search for potent urease inhibitors has attracted major scientific attention in recent years (see Scheme 1).

Tryptamine belongs to the class of monoamine alkaloids. It contains an indole ring. Tryptamine is derived through the decarboxylation of

* Corresponding authors at: H. E. J. Research Institute of Chemistry, International Center for Chemical and Biological Sciences, University of Karachi, Karachi 75270, Pakistan.
E-mail addresses: khalid.khan@iccs.edu (K.M. Khan), Iqbal.choudhary@iccs.edu (M.I. Choudhary).

https://doi.org/10.1016/j.bioorg.2018.10.070
Received 11 July 2018; Received in revised form 25 October 2018; Accepted 31 October 2018
Available online 01 November 2018

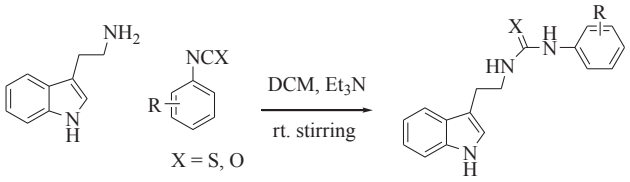

Scheme 1. Syntheses of urea and thiourea derivatives of tryptamine (**1–25**).

amino acid tryptophan. Tryptamine and its derivatives are known as hallucinogens, and possess various biological activities, such as anti-ulcerogenic [13], antihepatitis [14], and antioxidant properties [15]. Urease inhibitors can be classified into four major groups on the basis of their chemical structures; thiolate compounds that reacts with metallic site of the enzyme, hydroxamic acid and its derivatives which compete with urea for binding at the active site of enzyme, substituted phosphodiamidates, and some peptides chains ligands or chelators which bind with the nickel of urease [12].

Our research group has been engaged in search of new classes of urease inhibitors since last decade [16–19]. We have worked previously on compounds which are structurally similar to urea and thiourea *e.g.* semicarbazone and thiosemicarbazone [20], and reported their urease inhibition activity. In literature the synthetic tryptamines containing oxadiazole and triazole rings are reported to possess urease inhibitory activity [21]. Therefore, in view of the previous findings, we decided to synthesize urea and thiourea derivatives of tryptamine for the evaluation of their urease inhibitory activity, and encouraging results were obtained. To the best of our knowledge, fifteen compounds (**5–13**, **15**, **19–21**, **23**, **25**) are new, while compounds **1–4**, **14**, **16–18**, **22**, and **24** were reported previously [22–24] (Figs. 1 and 2).

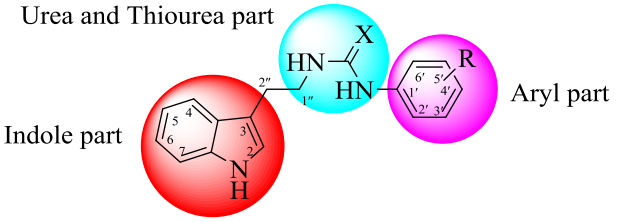

Fig. 2. General structure of tryptamine derivatives.

2. Results and discussion

2.1. Chemistry

Tryptamine (1 mmol) was taken in a reaction flask along with dichloromethane (20 mL) and *tri*ethylamine (0.5 mL) then different substituted isocyanates or isothiocyanates (1 mmol) were added to the reaction flask, and reaction mixture was stirred for 24 h. The progress was monitored with TLC. Upon consumption of the reactants, the solvent was evaporated, and residues obtained were washed with hexane to obtain products (Table 1). The synthetic derivatives were characterized by different spectroscopic techniques, such as EI-MS, HR EI-MS, ^{1}H NMR, and ^{13}C NMR spectroscopic techniques. Structure elucidation of one of the compounds is presented here as example.

2.2. Spectral characterization of tryptamine derivatives

2.2.1. ^{1}H NMR spectroscopy

The ^{1}H NMR spectrum of most active compound **14** is presented here. The spectrum was recorded in DMSO-d_6 on a 400 MHz

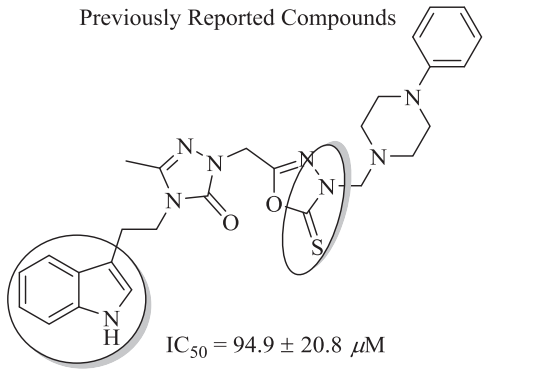

IC_{50} = 94.9 ± 20.8 μM

4-(2-(1*H*-indol-3-yl)ethyl)-5-methyl-2-((4-((4-phenylpiperazin-1-yl)methyl)-5-thioxo-4,5-dihydro-1,3,4-oxadiazol-2-yl)methyl)-2,4-dihydro-3*H*-1,2,4-triazol-3-one

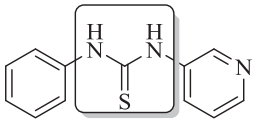

1-phenyl-3-(pyridin-3-yl)thiourea

IC_{50} = 8.43 ± 0.02 μM

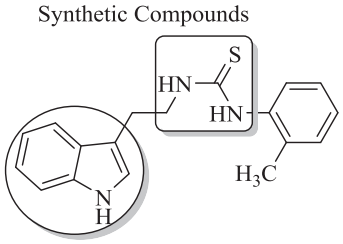

1-(2-(1*H*-indol-3-yl)ethyl)-3-(*o*-tolyl)thiourea

IC_{50} = 11.4 ± 0.4 μM

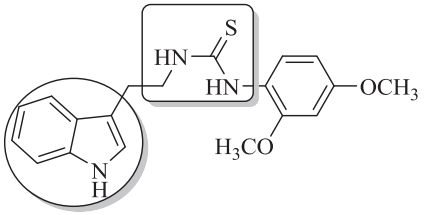

1-(2-(1*H*-indol-3-yl)ethyl)-3-(2,4-dimethoxyphenyl)thiourea

IC_{50} = 13.2 ± 0.9 μM

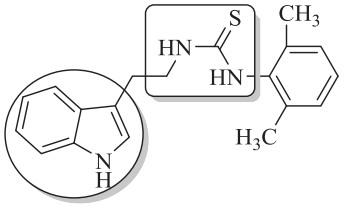

1-(2-(1*H*-indol-3-yl)ethyl)-3-(2,6-dimethylphenyl)thiourea

IC_{50} = 12.8 ± 0.47 μM

Fig. 1. Rationale of current study.

Table 1
Urea and thiourea analogues of tryptamine 1–25.

Compound	R
Urea derivatives	
1	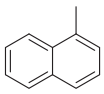
2	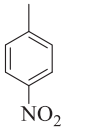
3	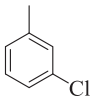
4	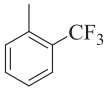
5	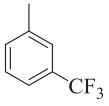
Thiourea derivatives	
6	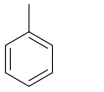
7	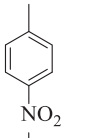
8	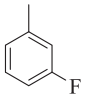
9	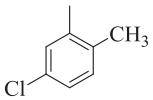
10	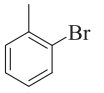
11	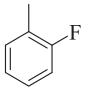
12	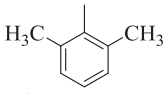
13	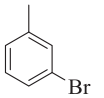
14	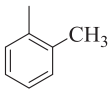
15	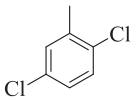
16	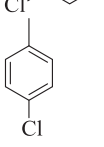

Table 1 (*continued*)

Compound	R
17	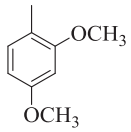
18	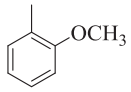
19	
20	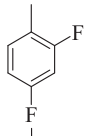
21	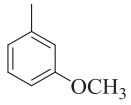
22	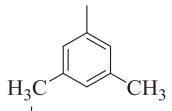
23	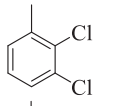
24	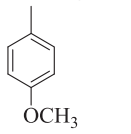
25	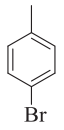

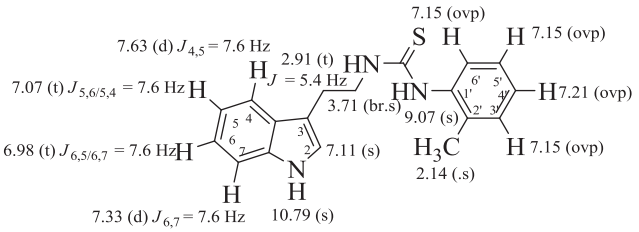

Fig. 3. ^{1}H NMR chemical shifts of compound **14**.

instrument. The most downfield signal resonated at δ_H 10.79 as a sharp singlet was due to indole NH. Another sharp singlet at δ_H 9.07 represented thiourea NH. The molecule comprises of nine aromatic protons, H-4 appeared as a doublet at δ_H 7.63 ($J_{4,5}$ = 7.6 Hz), while H-7 appeared at δ_H 7.33 as a doublet ($J_{7,6}$ = 7.6 Hz). Multiplets for H-3′, H-5′, and H-6′ were overlapped at δ_H 7.15. A singlet for H-2 appeared at δ_H 7.11, while H-5 resonated at δ_H 7.07 as a triplet ($J_{5,6/5,4}$ = 7.6 Hz). H-6 of indole was resonated as a triplet at δ_H 6.98 ($J_{6,7/6,5}$ = 7.6 Hz). The CH_3 protons resonated at δ_H 2.14 as a singlet. Chemical shifts of remaining protons are shown on Fig. 3.

The ^{13}C NMR (broad-band decoupled) spectrum (DMSO-d_6) showed a total of 16 carbon signals, including one methyl, two methylene, nine methine, and four quarternary carbons. The most downfield signal was of thiocarbonyl group at δ_C 180.8. Quarternary C-2′ and C-9 were

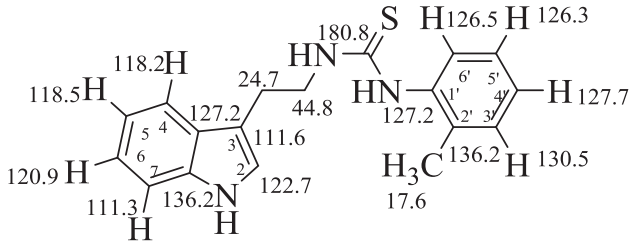

Fig. 4. ^{13}C NMR chemical shifts in compound **14**.

resonated at δ_C 136.2. Whereas, methine C-3′ and C-4′ appeared at δ_C 130.5 and 127.7, respectively. All remaining aromatic carbons appeared in the usual aromatic range of δ_C 111.3–136.2. The methylene carbon, adjacent to electronegative nitrogen atom, appeared at δ_C 44.8, while the adjacent methylene carbon resonated at δ_C 24.7. The most upfield carbon was of methyl that appeared at δ_C 17.6. The ^{13}C NMR chemical shifts of the compound **14** are shown in Fig. 4.

2.2.2. Mass spectrometry

The EI-MS spectra of compound **14** showed the M^+ at *m/z* 309, in agreement with $C_{18}H_{19}N_3S$ (309.1300 a.m.u.). The ion at *m/z* 143 represented 3-ethyl indole ion as the base peak. The fragment at *m/z* 129 was due to the formation of 3-methyl indole, while fragment at *m/z* 150 was due to the loss of methyl group from isothiocyanate radical ion. The key fragments are presented in Fig. 5.

2.3. Bioactivities

2.3.1. Structure-activity relationship

Compounds **1–25** were evaluated for their urease inhibitory activity. Five compounds **8**, **10**, **18**, **21**, and **21** showed comparable activity with that of standard thiourea, nine compounds **11–17**, **22**, and **24** showed potent activity, while rest of the compounds were inactive (Table 2).

Limited structure-activity relationship proposed that the activity of this series is mostly dependent on the nature and position of substituents. The molecules having CH_3 and OCH_3 were found to be most potent members of the series. Compound **14** with a methyl at *ortho* position was the most active member (IC_{50} = 11.4 ± 0.4 μM). The *ortho di*-methyl substituted derivative **12** was the second most active compound (IC_{50} = 12.8 ± 0.5 μM). Whereas, the *meta di*-methyl substituted compound **22** (IC_{50} = 19.7 ± 0.7 μM) showed a lower activity due to shifting of the position of *ortho* substituent to *meta* substituent.

Table 2
Urease inhibitory activity (IC_{50} in μM) of compounds **1–25**.

Compound	IC_{50} ± SEM[a] (μM)
Urea derivatives	
1	N.A.[b]
2	N.A.[b]
3	N.A.[b]
4	N.A.[b]
5	N.A.[b]
Thiourea derivatives	
6	N.A.[b]
7	N.A.[b]
8	21.3 ± 1.5
9	N.A.[b]
10	24.2 ± 1.5
11	14.5 ± 0.57
12	12.8 ± 0.47
13	16.6 ± 1.4
14	11.4 ± 0.4
15	17.1 ± 1.0
16	13.7 ± 0.9
17	13.2 ± 0.9
18	23.7 ± 0.22
19	27.1 ± 0.64
20	N.A.[b]
21	23.0 ± 0.83
22	19.7 ± 0.7
23	N.A.[b]
24	14.2 ± 0.6
25	N.A.[b]
Thiourea[(std)]	21.2 ± 1.2

[a] SEM is the standard error of the mean.
[b] NA Not active; Thiourea [(std)] standard inhibitor for urease inhibitory activity.

Among halogen substituted derivatives, the *para* substituted chloro containing compound **16** was the most active with IC_{50} = 13.7 ± 0.9 μM. Comparison of compounds **16** with **19** indicated that the change of chloro group from *para* to *ortho* resulted in a sharp decline in activity of compound **19** (IC_{50} = 27.1 ± 0.64 μM). Similarly, compounds **11** (IC_{50} = 14.5 ± 0.57 μM) and **10** (IC_{50} = 24.2 ± 1.5 μM) having fluoro and bromo substituents at *ortho* and *meta* positions, respectively, also showed less activity, as compared to compound **16**.

2.3.2. Methyl substituted compounds

The most active compound **14** (IC_{50} = 11.4 ± 0.4 μM) possess a

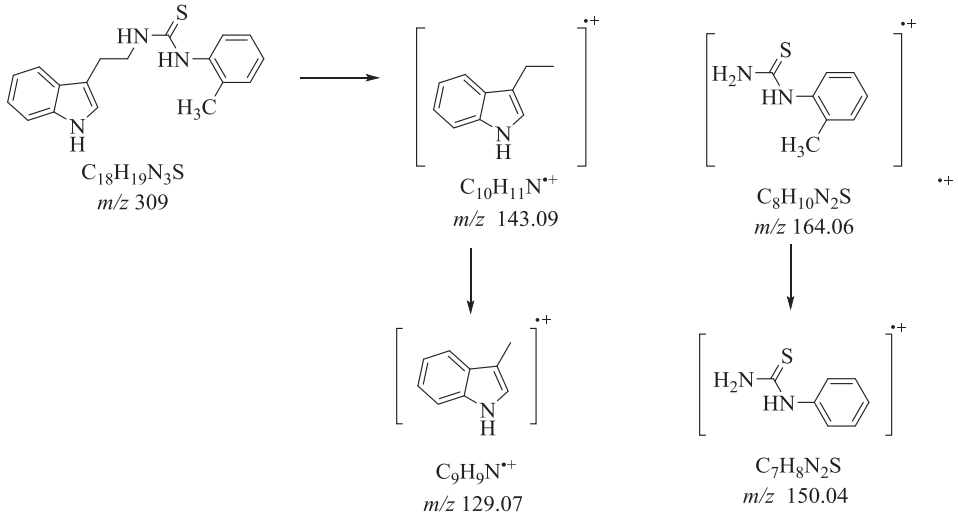

Fig. 5. Key fragmentation pattern (HREI-MS) of compound **14**.

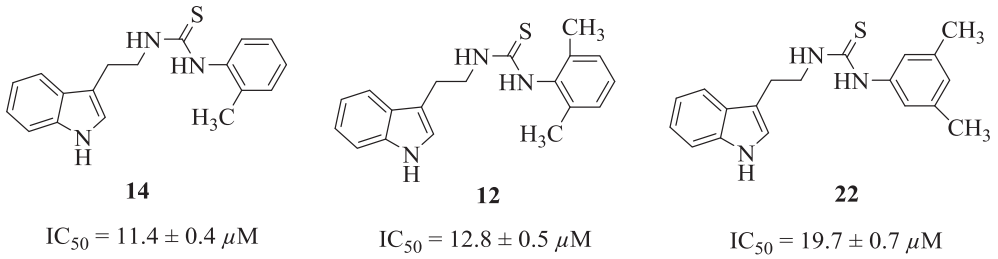

Fig. 6. Methyl substituent effect on urease inhibitory activity.

methyl group at the *ortho* position. When its activity was compared with *di-ortho* methyl substituted compound **12** (IC_{50} = 12.8 ± 0.5 μM), no profound difference was observed. However, activity decreased when the methyl substituents were substituted on *meta*, as in compound **22** (IC_{50} = 19.7 ± 0.7 μM) (Fig. 6).

2.3.3. Methoxy substituted compounds

Compound **24** (IC_{50} = 14.2 ± 0.6 μM) having a methoxy substituent at *para* position may be responsible for its good activity. While compounds **21** (IC_{50} = 23.0 ± 0.8 μM) and **18** (IC_{50} = 23.7 ± 0.22 μM) showed a slightly lower activity due to change in the position of methoxy to *meta* and *ortho,* respectively. Whereas, the *di*-substituted analogue **17** (IC_{50} = 13.2 ± 0.9 μM) showed a potent activity as compared to standard (thiourea), along derivatives **24**, **21**, and **18**, where methoxy groups were at *para* and *ortho* positions (Fig. 7).

2.3.4. Halogen substituted compounds

Among halogen substituted derivatives, compound **16** (IC_{50} = 13.7 ± 0.9 μM) was the most active one as it possess chloro group at *para* position. Compound **11** (IC_{50} = 14.5 ± 0.5 μM) having a flouro group at *ortho* position showed a potent activity as compared to standard thiourea, whereas compound **8** (IC_{50} = 21.3 ± 1.5 μM) also possess a fluorine but it was less active than compound **11**. This may be due to change in position of fluorine from *ortho* to *meta* position. Compound **19** (IC_{50} = 27.1 ± 0.6 μM) was less active as compared to compound **16** by just changing the position of chlorine substituent from *para* to *ortho*. However, compound **15** (IC_{50} = 17.1 ± 1.0 μM) with *di*-chloro groups at *ortho* and *meta* positions, also showed a lower activity as compared to compound **16**. This indicated that substitution at *meta* position cause a decrease in activity. Among the bromo substituted derivatives, compound **13** (IC_{50} = 16.6 ± 1.4 μM) possess a good activity. Whereas, *ortho* substituted bromo group led to a decreased activity, as in compound **10** (IC_{50} = 24.2 ± 1.5 μM) (Fig. 8).

2.3.5. Cytotoxicity evaluation

All synthetic compounds **1–25** were evaluated for their cytotoxicity, and found to be non-cytotoxic against the mouse fibroblast 3T3 cell line, in comparison to the standard cycloheximide.

2.3.6. Kinetic studies

The kinetic studies determined the mechanism of action of the most active compounds, using urease as a substrate. Lineweaver–Burk plot (the reciprocal of the substrate concentration *1/V* and the reciprocal of the rate of the reaction *1/S*) were used for determining the inhibition type, and to study the effect of inhibitor on both *Km* and *Vmax*. The *Ki* values were determined by plotting the slope *Km/Vmax* of each line in the Lineweaver–Burk plots against different concentrations of compounds. Kinetic studies on compounds **8** and **13** showed a mixed mode of inhibition. Compounds **11**, **12**, **14**, **17**, **18**, **21**, **22**, and **24** showed that these compounds inhibit the urease in non-competitive manner (Table 3 and Figs. 9–18).

2.3.7. Molecular docking studies

All of the thiourea derivatives of tryptamine acquired different poses in the allosteric site of jack bean urease (*EC 3.5.1.5*). Compound **8** interacted with Asp730 *via* hydrogen bonding through its thiourea moiety, while tryptamine moiety form hydrogen bonding with Glu718 residue (Fig. 19a). Compound **11** forms hydrogen bond interaction with Lys716 through its thiourea moiety, while its tryptamine moiety was engaged in π-cation and π-π interactions with Lys716 and Phe838, respectively (Fig. 19b). Compound **12** exhibited hydrogen bonding to

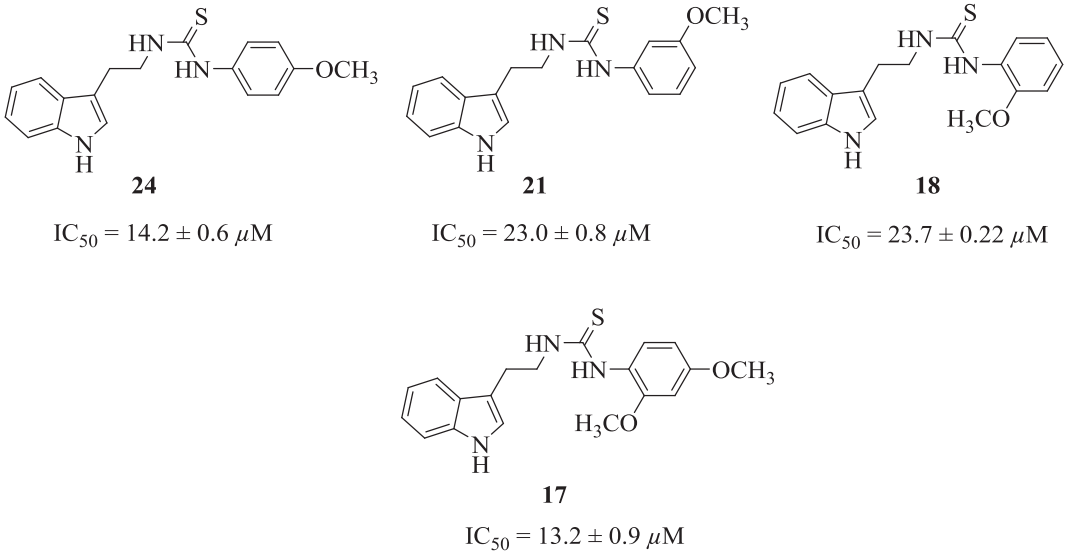

Fig. 7. Effect of methoxy substituents on urease inhibitory activity.

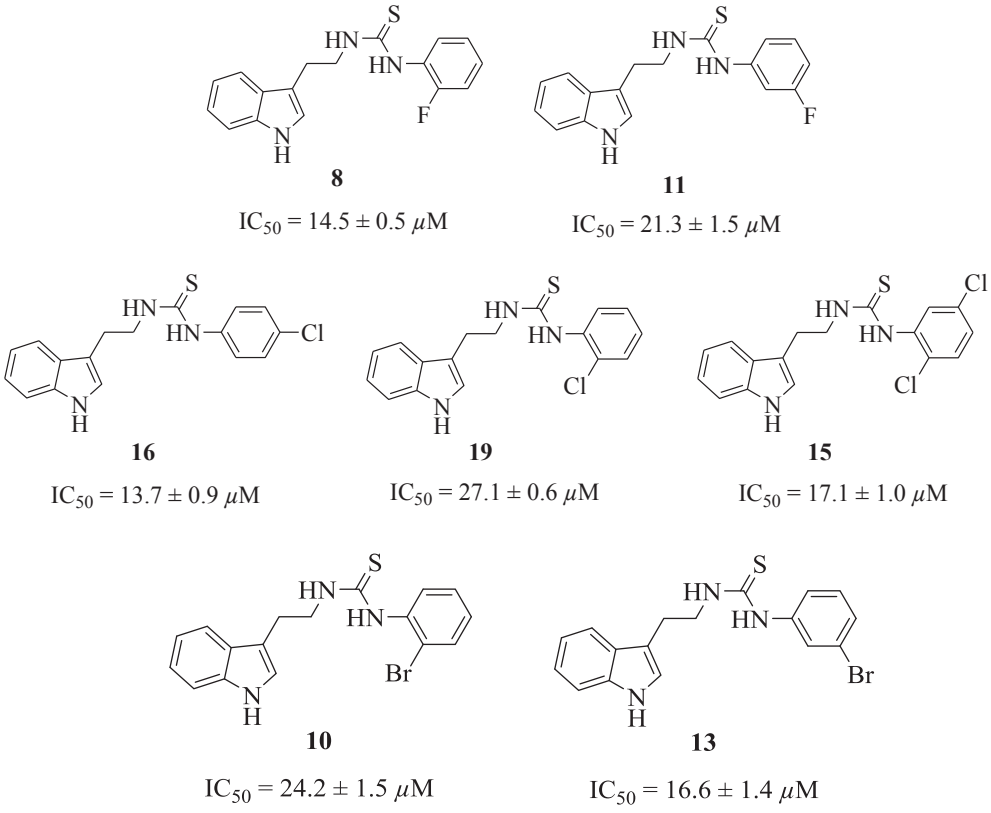

Fig. 8. Effect of halogen substituents on urease inhibitory activity.

Table 3
Kinetic data of selected urease inhibitors.

Compound	*Ki*[a] + SEM[b] (μM)	Type of inhibition
8	20.0 ± 0.001	Mixed inhibition
11	18.8 ± 0.025	Non-competitive inhibition
12	12.0 ± 0.001	Non-competitive inhibition
13	17.4 ± 0.001	Mixed inhibition
14	11.7 ± 0.007	Non-competitive inhibition
17	19.9 ± 0.001	Non-competitive inhibition
18	21.3 ± 0.001	Non-competitive inhibition
21	17.0 ± 0.018	Non-competitive inhibition
22	21.7 ± 0.001	Non-competitive inhibition
24	16.3 ± 0.009	Non-competitive inhibition
Thiourea standard	21.0 ± 0.002	Competitive inhibition

[a] *Ki* is Dissociation constant.
[b] SEM is the Standard Error of the Mean.

Asp730 through its thiourea moiety. Two hydrogen bonds were also observed *via* Glu418 through the tryptamine moiety (Fig. 19c). Compound **13** exhibited same non-covalent interaction pattern and pose as that of compound **8**. It made hydrogen bonding with Asp730 and Glu718 *via* its tryptamine and thiourea moieties, respectively. The similarity in interactions and poses can be attributed to the halogen substitution *i.e.,* bromo at the *meta* position (Fig. 19d). Compound **14** with *ortho* methyl substitution at benzyl group interacted to Val744 and Ser421 through its thiourea and tryptamine moieties, respectively (Fig. 19e).

Compound **17** interacted *via* its tryptamine moiety, and *ortho* methoxy substitution at benzyl moiety. A hydrogen bond was observed between Glu718 of allosteric site and tryptamine moiety, while the other hydrogen bond was between Met746 and *ortho* methoxy group (Fig. 20a). Compound **18** with *mono* methoxy substitution at *ortho* position retained the same interaction with Met746 as that of compound **17**. However, a change in interaction pattern was observed for tryptamine moiety. It form a hydrogen bond with another Glu residue at 742 position (Fig. 20b). Compound **21** with *meta* methoxy substitution was involved in hydrogen bonding *via* its thiourea moiety to Glu418 (Fig. 20c). In case of compound **22** the thoiurea moiety was involved in forming hydrogen bonds with Lys716, Asp730, Val744, and Thr715. While the tryptamine moiety was involved in π-π and π-cation interactions with Phe838, and Lys716, respectively. Lys716 made another π-cation interaction with the *di*methyl substituted benzyl moiety of compound **22** (Fig. 20d). Compound **24** had only one hydrogen bonding with Glu718 *via* its tryptamine moiety (Fig. 20e).

Docking of thiourea derivatives of tyramine in allosteric site revealed that the substitution with different functional groups on benzyl moiety make them acquire different poses. It can be seen in most of the derivatives, tryptamine and thiourea moieties were interacting with the allosteric site residues, while adopting an altered pose.

3. Materials and methods

^{1}H- and ^{13}C NMR spectra were recorded on 300 and 400 MHz spectrometers (Bruker Avance, Switzerland). Mass experiments were carried out on a Finnigan MAT-311A (Germany) mass spectrometer. Thin-layer chromatography (TLC) was carried out on pre-coated silica gel aluminum plates (Kieselgel 60, 254, E. Merck, Germany). Visualization of TLC chromatograms was performed by UV light at wavelengths of 254 and 365 nm. Dichloromethane (CH_2Cl_2) of analytical grade was used (RCI Labscan Limited, Thailand). *Tri*ethylamine and all isocyanates and isothiocyanates were of analytical grades, and used as received from Wako, Japan. Tryptamine was purchased from Merck, Germany.

3.1. Urease inhibition assay

Urease enzyme (Jack bean, *Canavalia ensiformis*, *EC 3.5.1.5*) 25 μL with 55 μL of buffer and 100 mM urea were incubated with 5 μL of test

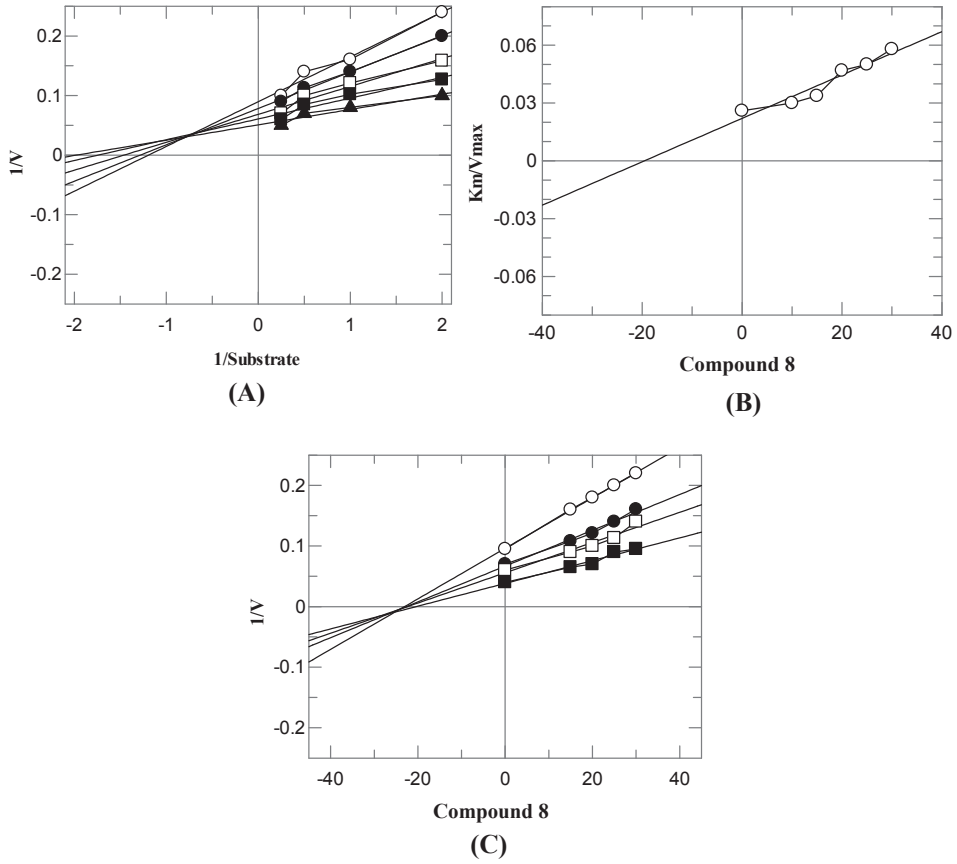

Fig. 9. Urease inhibition by compound 8, (A) Lineweaver-Burk plot of reciprocal rate of reaction *1/V* against reciprocal of substrate *1/S* (urea) in the absence (▲) and in the presence of 5 μM (Δ), 10 μM (■), 15 μM (□), 20 μM (●) 25 μM (○) of compound 8. (B) Is the secondary replot is the reciprocal of slope *vs* different concentrations of compound 8, and (C) Dixon plot reciprocal of rate of reaction *vs* different concentrations of compound **8**.

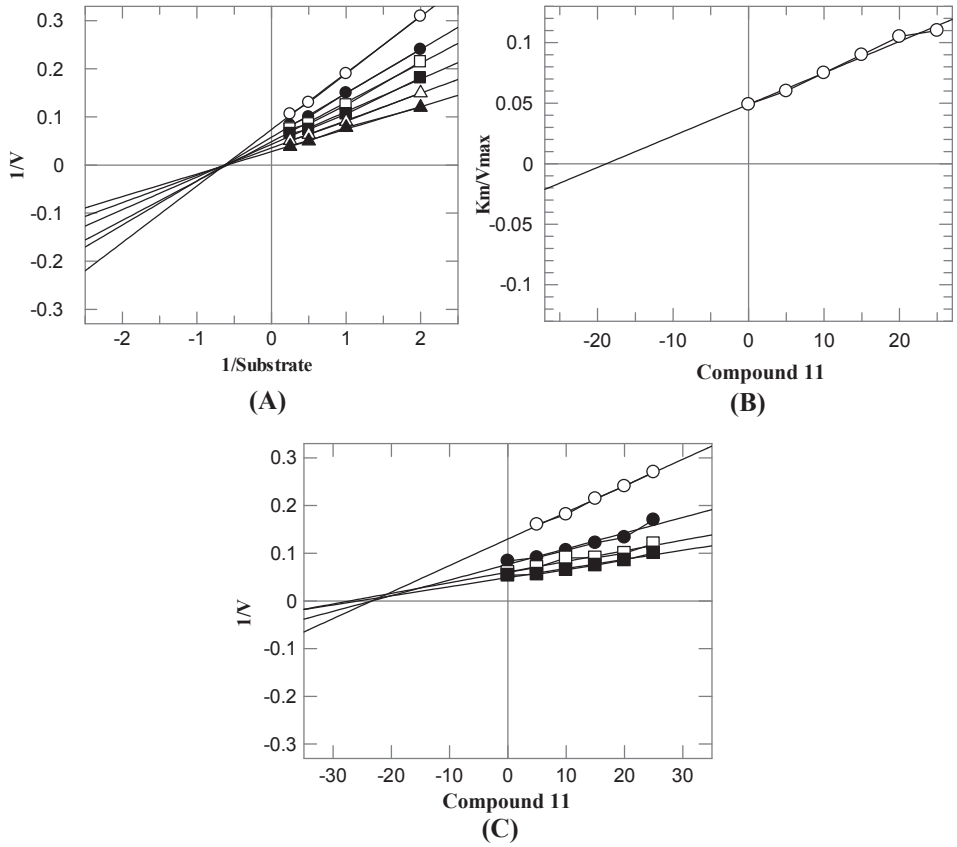

Fig. 10. Urease inhibition by compound **11**, (A) Lineweaver-Burk plot of reciprocal rate of reaction *1/V* against reciprocal of substrate *1/S* (urea) in the absence (▲) and in the presence of 5 μM (Δ), 10 μM (■), 15 μM (□), 20 μM(●) 25 μM (○) of compound **11**. (B) Is the secondary replot is the reciprocal of slope *vs* different concentrations of compound **11**, and (C) Dixon plot reciprocal of rate of reaction *vs* different concentrations of compound **11**.

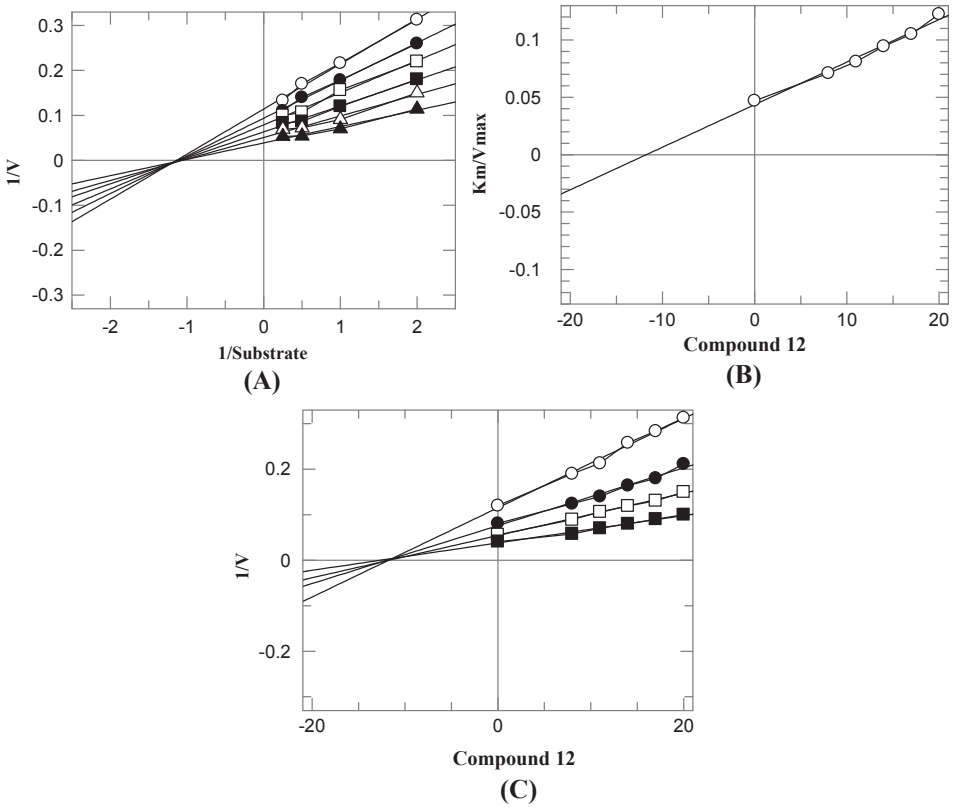

Fig. 11. Urease inhibition by compound **12**, (A) Lineweaver-Burk plot of reciprocal rate of reaction *1/V* against reciprocal of substrate *1/S* (urea) in the absence (▲) and in the presence of 5 μM (Δ), 10 μM (■), 15 μM (□), 20 μM (●) 25 μM (○) of compound **12**. (B) Is the secondary replot is the reciprocal of slope *vs* different concentrations of compound **12**, and (C) Dixon plot reciprocal of rate of reaction *vs* different concentrations of compound **12**.

compounds at 30 °C for 15 min in 96-well plates. Weatherburn indophenol method was used to determine urease inhibitory activity by measuring ammonia production [25]. Briefly, 45 μL each phenol reagent (1% w/v phenol and 0.005% w/v sodium nitroprusside) and 70 μL of alkali reagent (0.5% w/v NaOH and 0.1% active chloride NaOCl) were added to each well. The increasing absorbance at 630 nm was measured after 50 min, using a microplate reader (Molecular Devices, USA). All reactions were performed in triplicate (as a result final

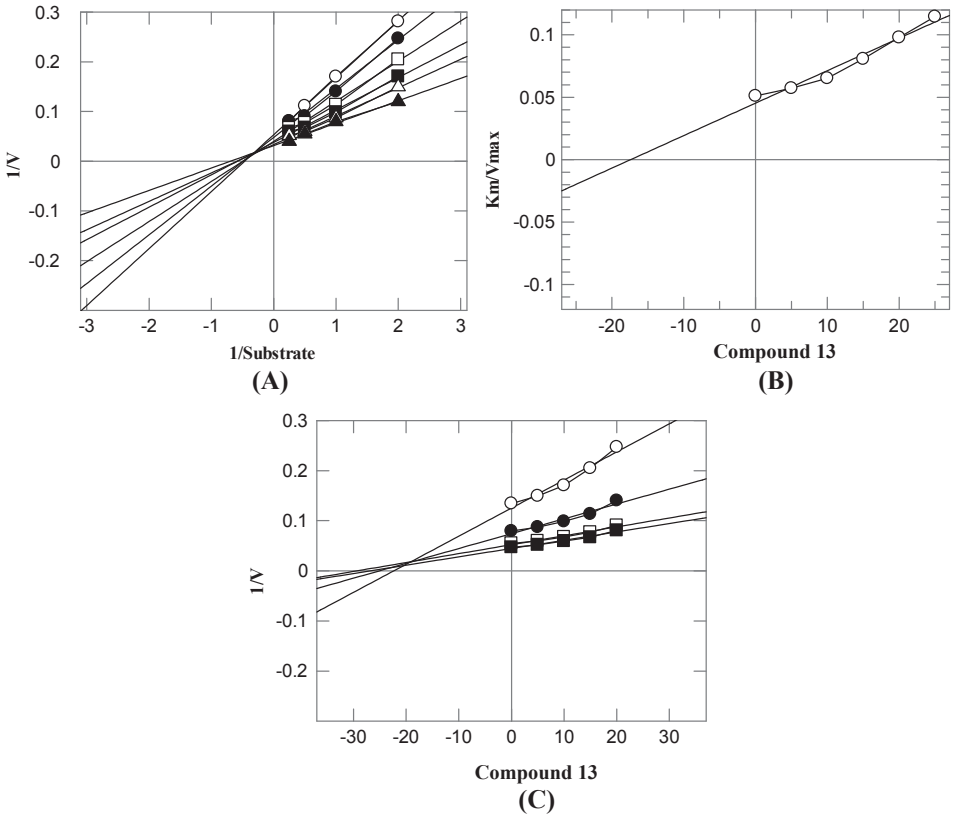

Fig. 12. Urease inhibition by compound **13**, (A) Lineweaver-Burk plot of reciprocal rate of reaction *1/V* against reciprocal of substrate *1/S* (urea) in the absence (▲) and in the presence of 5 μM (Δ), 10 μM (■), 15 μM (□), 20 μM (●) 25 μM (○) of compound **13**. (B) Is the secondary replot is the reciprocal of slope *vs* different concentrations of compound **13**, and (C) Dixon plot reciprocal of rate of reaction *vs* different concentrations of compound **13**.

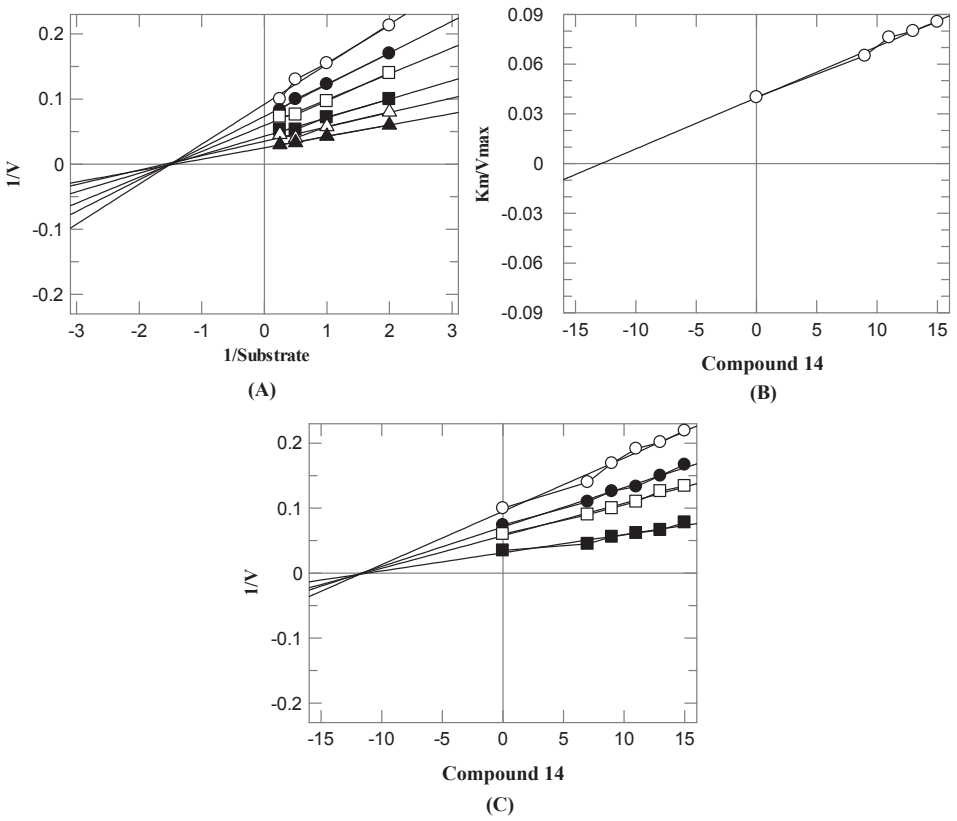

Fig. 13. Urease inhibition by compound **14**, (A) Lineweaver-Burk plot of reciprocal rate of reaction *1/V* against reciprocal of substrate *1/S* (urea) in the absence (▲) and in the presence of 5 μM (Δ), 10 μM (■), 15 μM (□), 20 μM (●) 25 μM (○) of compound **14**. (B) Is the secondary replot is the reciprocal of slope *vs* different concentrations of compound **14**, and (C) Dixon plot reciprocal of rate of reaction *vs* different concentrations of compound **14**.

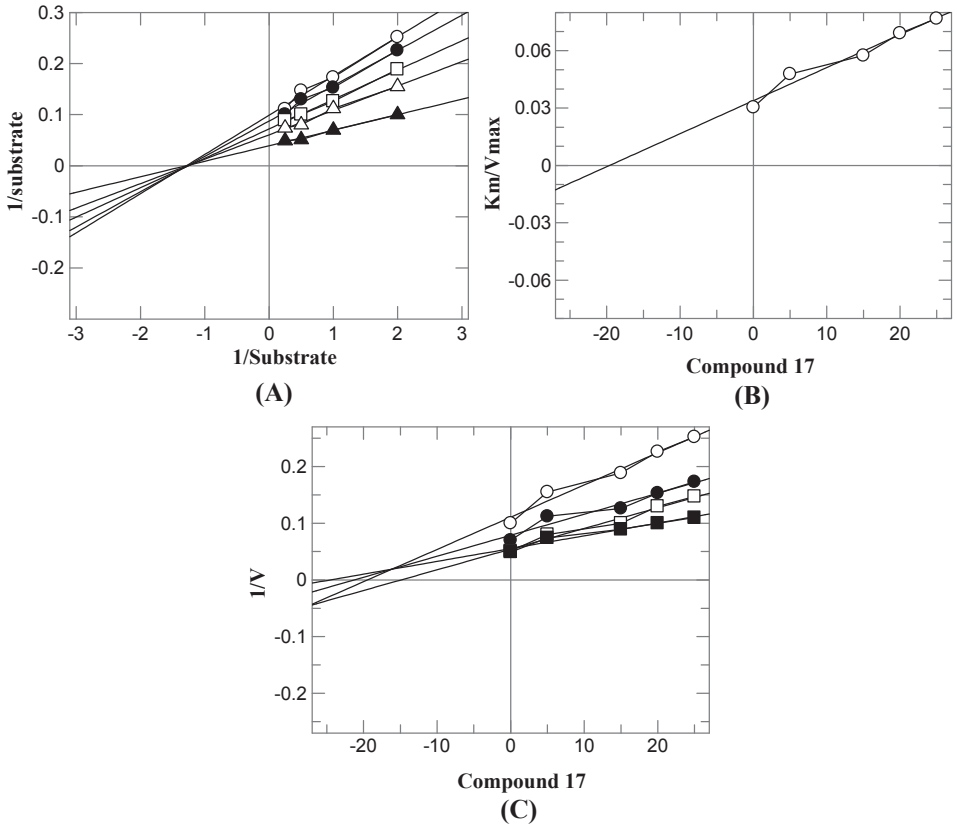

Fig. 14. Urease inhibition by compound **17**, (A) Lineweaver-Burk plot of reciprocal rate of reaction *1/V* against reciprocal of substrate *1/S* (urea) in the absence (▲) and in the presence of 5 μM (Δ), 10 μM (■), 15 μM (□), 20 μM (●) 25 μM (○) of compound **17**. (B) Is the secondary replot is the reciprocal of slope *vs* different concentrations of compound **17**, and (C) Dixon plot reciprocal of rate of reaction *vs* different concentrations of compound **17**.

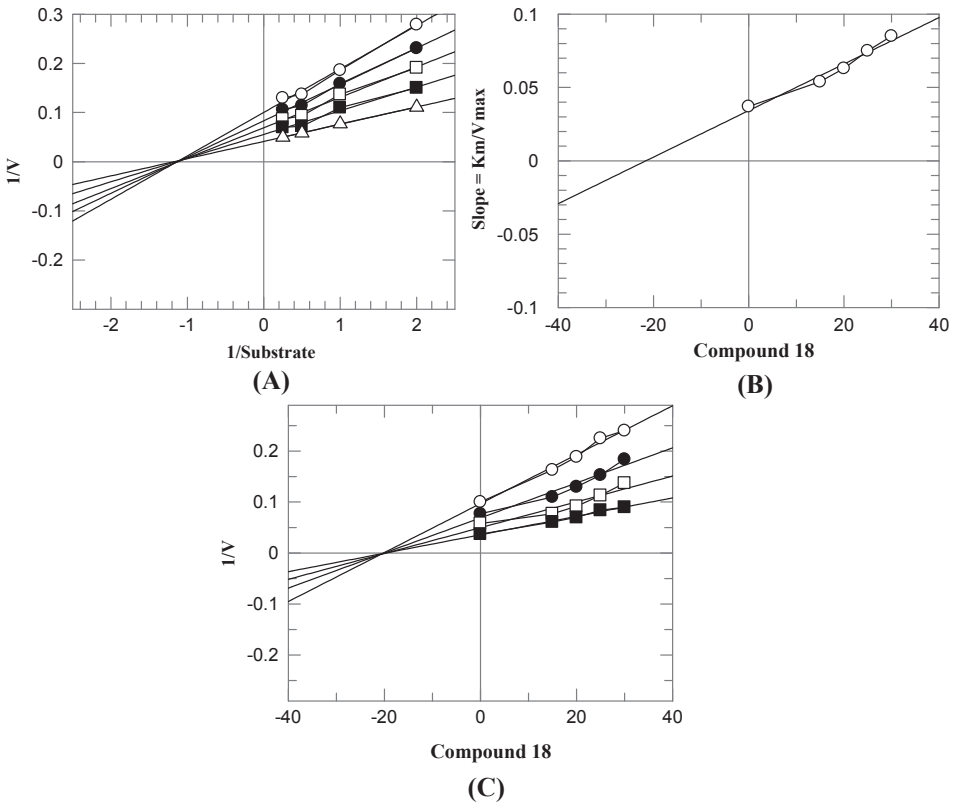

Fig. 15. Urease inhibition by compound **18**, (A) Lineweaver-Burk plot of reciprocal rate of reaction *1/V* against reciprocal of substrate *1/S* (urea) in the absence (▲) and in the presence of 5 μM (Δ), 10 μM (■), 15 μM (□), 20 μM (●) 25 μM (○) of compound **18**. (B) Is the secondary replot is the reciprocal of slope *vs* different concentrations of compound **18**, and (C) Dixon plot reciprocal of rate of reaction *vs* different concentrations of compound **18**.

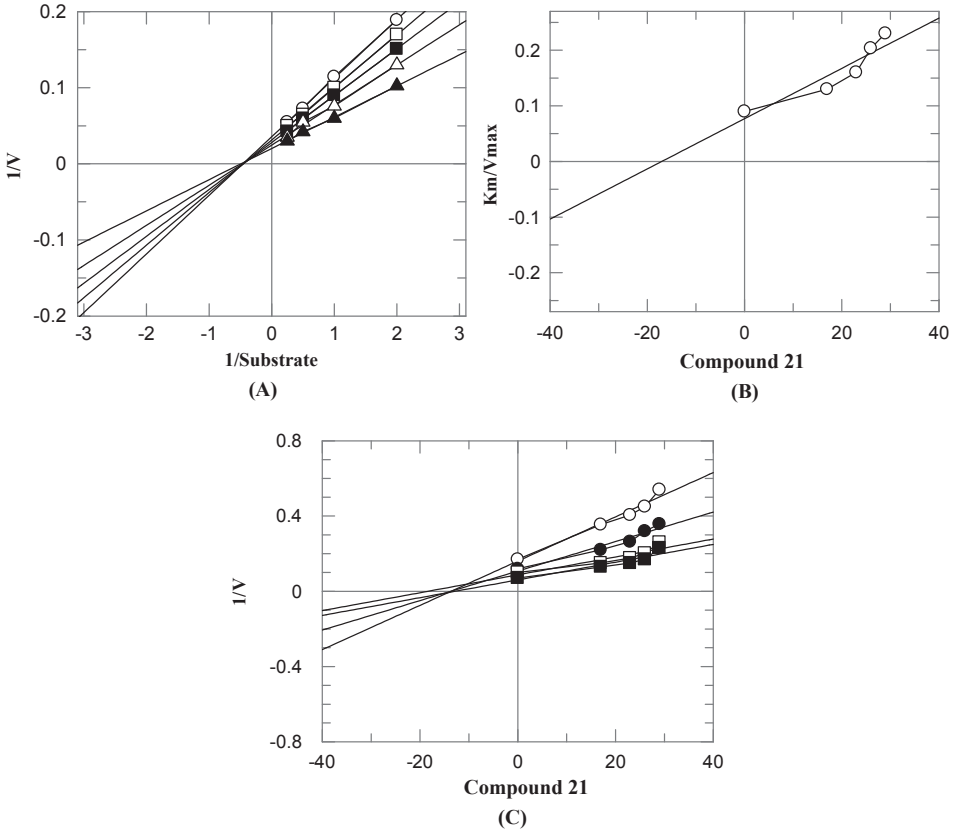

Fig. 16. Urease inhibition by compound **21**, (A) Lineweaver-Burk plot of reciprocal rate of reaction *1/V* against reciprocal of substrate *1/S* (urea) in the absence (▲) and in the presence of 5 μM (Δ), 10 μM (■), 15 μM (□), 20 μM (●) 25 μM (○) of compound **21**. (B) Is the secondary replot is the reciprocal of slope *vs* different concentrations of compound **21**, and (C) Dixon plot reciprocal of rate of reaction *vs* different concentrations of compound **21**.

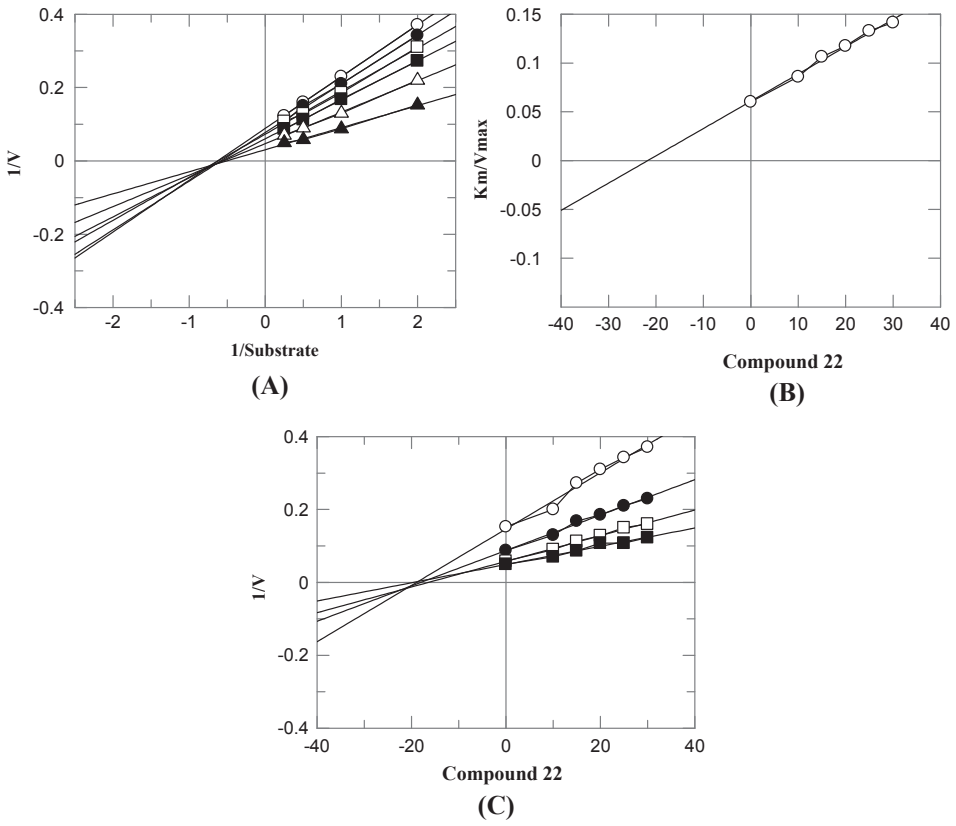

Fig. 17. Urease inhibition by compound **22**, (A) Lineweaver-Burk plot of reciprocal rate of reaction *1/V* against reciprocal of substrate *1/S* (urea) in the absence (▲) and in the presence of 5 μM (Δ), 10 μM (■), 15 μM (□), 20 μM (●) 25 μM (○) of compound **22**. (B) Is the secondary replot is the reciprocal of slope *vs* different concentrations of compound **22**, and (C) Dixon plot reciprocal of rate of reaction *vs* different concentrations of compound **22**.

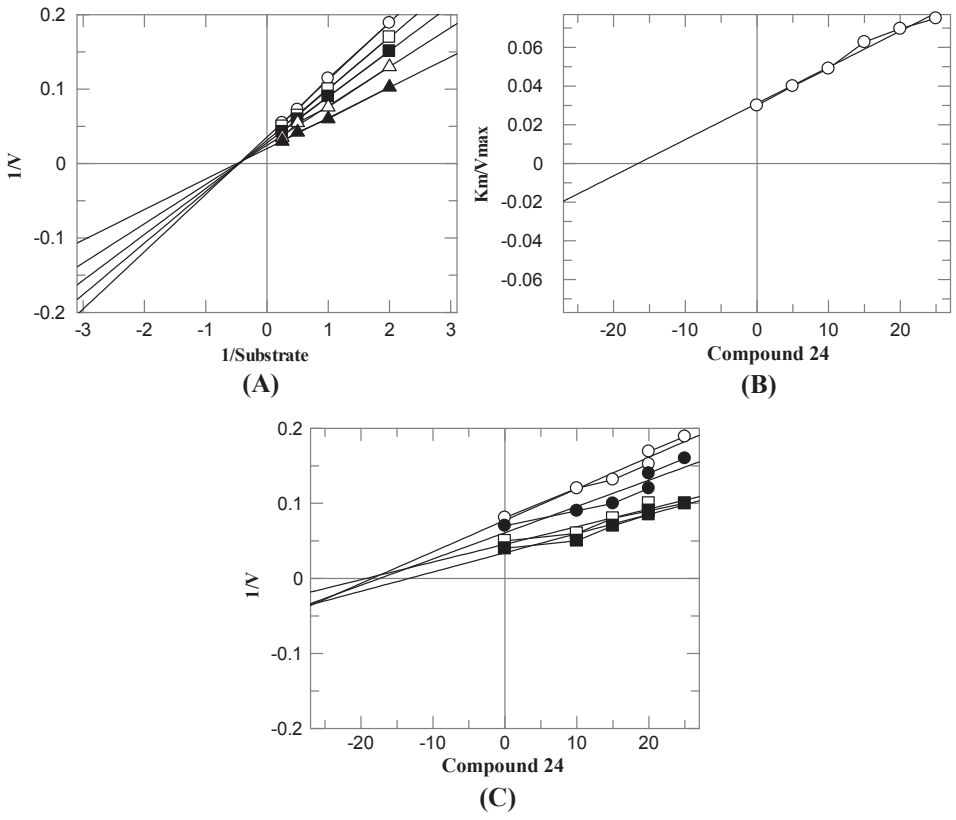

Fig. 18. Urease inhibition by compound **24**, (A) Lineweaver-Burk plot of reciprocal rate of reaction *1/V* against reciprocal of substrate *1/S* (urea) in the absence (▲) and in the presence of 5 μM (Δ), 10 μM (■), 15 μM (□), 20 μM (●) 25 μM (○) of compound **24**. (B) Is the secondary replot is the reciprocal of slope *vs* different concentrations of compound **24**, and (C) Dixon plot reciprocal of rate of reaction *vs* different concentrations of compound **24**.

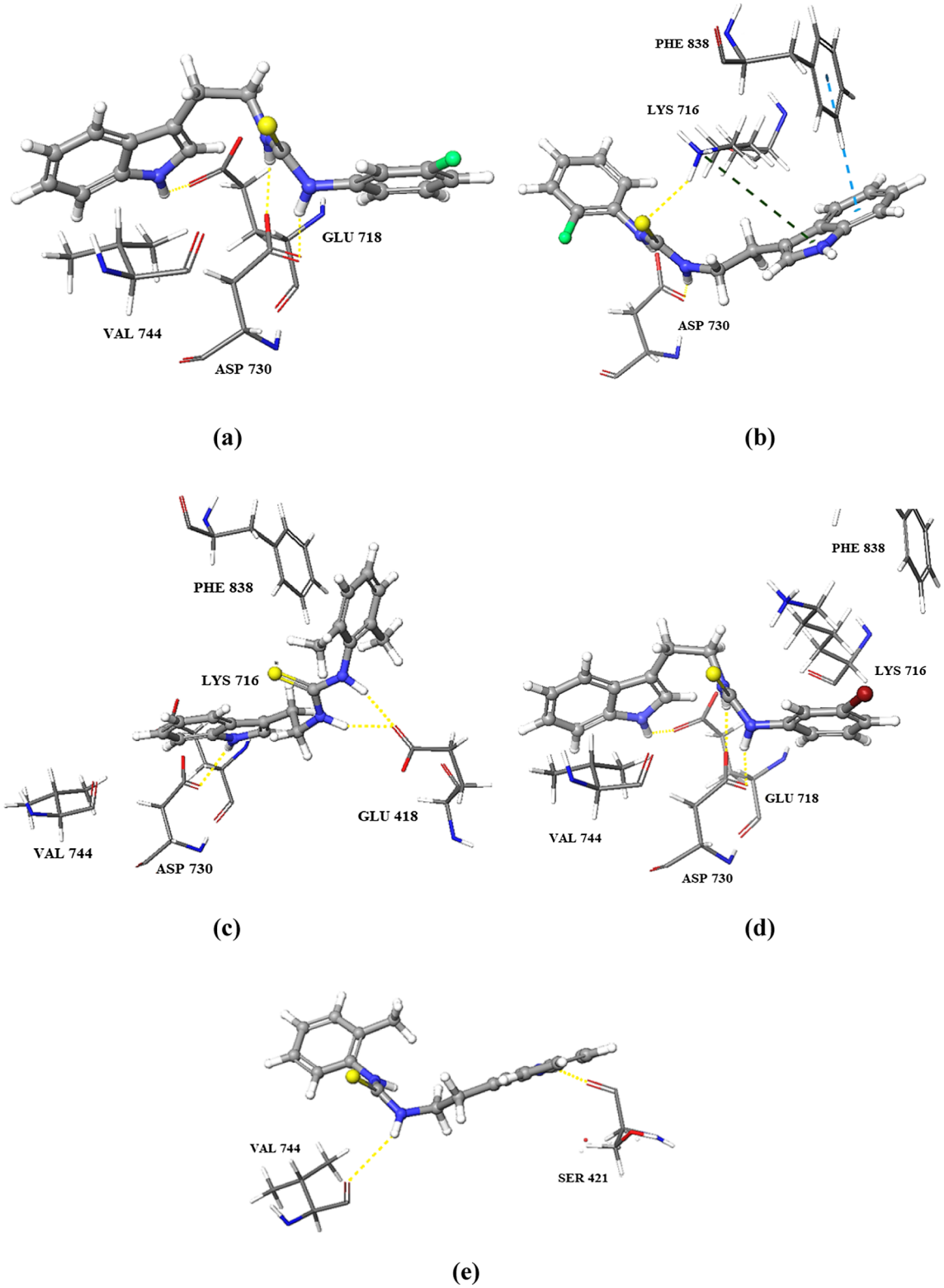

Fig. 19. Modelled thiourea derivatives of tyramine in allosteric site of Jack bean urease (PDB ID: 4H9M). 3D view of modelled compounds (ball and stick) (a) 8, (b) 11, (c) 12, (d) 13, and (e) 14 in allosteric site with residues of enzyme represented by sticks. Hydrogen bonds, π-π, and π-cation interactions are shown as yellow, blue and green dotted lines, respectively. (For interpretation of the references to colour in this figure legend, the reader is referred to the web version of this article.)

volume was 200 µL). 20 Soft-Max Pro-Software (Molecular Devices, USA) was used to measure the change in absorbance with reference to time. The entire assay was performed at pH 6.8. Percentage inhibitions were calculated from the formula 100-(OD test well/OD control) × 100 and thiourea standard was used in this assay [26].

3.2. Cytotoxicity assay

The standard MTT (3-[4,5-dimethylthiazole-2-yl]-2,5-diphenyl-tetrazolium bromide) colorimetric assay was used for the evaluation of cytotoxic activity using 96-well flat-bottomed micro plates [27].

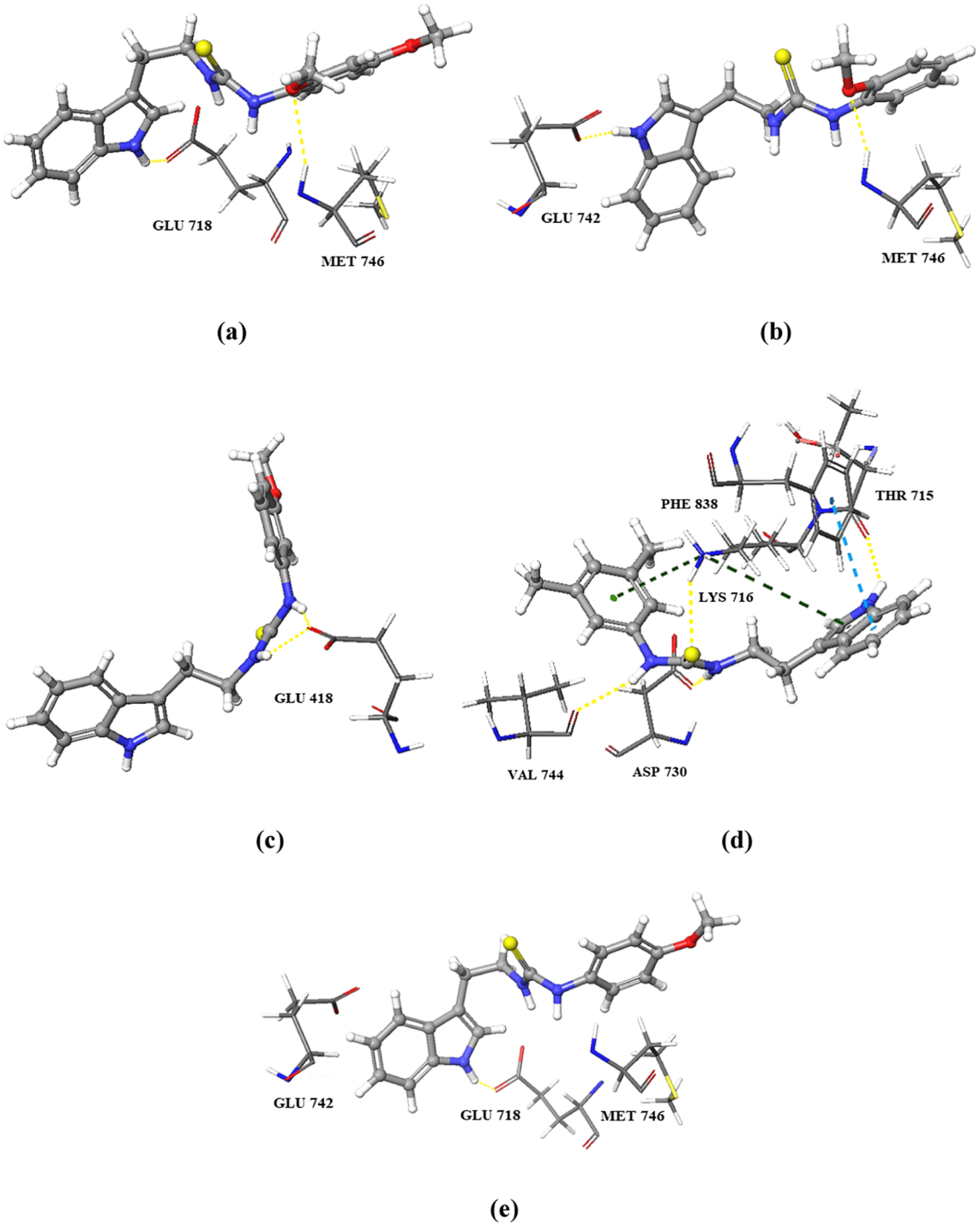

Fig. 20. Modelled thiourea derivatives of tyramine in allosteric site of Jack bean urease (PDB ID: 4H9M). 3D view of modelled compounds (ball and stick) (a) 17, (b) 18, (c) 21, (d) 22, and (e) 24 in allosteric site with residues of enzyme represented by sticks. Hydrogen bonds, π-π, and π-cation interactions are shown as yellow, blue and green dotted lines, respectively. (For interpretation of the references to colour in this figure legend, the reader is referred to the web version of this article.)

Dulbecco's Modified Eagle Medium was used for the culturing of 3 T3 (mouse fibroblast) cells, the medium was supplemented with 100 µg/mL of streptomycin, 5% of fetal bovine serum (FBS), and 100 IU/mL of penicillin in 75 cm^2 flasks. The medium was then incubated at 37 °C and kept in 5% CO_2. The exponentially grown cells were harvested, counted using haemocytometer and diluted with a particular medium. The cell culture was diluted upto a concentration of 5×10^4 cells/mL and transferred into 96-well plates. The medium was incubated overnight, the samples were prepared by using compounds with different concentrations (1–30 µM) and 200 µL of fresh medium was also added. The samples were incubated for 48 h, then 200 µL MTT (0.5 mg/mL) was added to each well, and incubated further for 4 h, 100 µL of DMSO was added to each well. Micro plate reader (Molecular Devices, CA, USA) was used for recording absorbance at 540 nm and the extent of MTT reduction to formazan within cells was calculated. The cytotoxicity was recorded as concentration causing 50% growth inhibition (IC_{50}) for 3 T3 cells [28]. The percent inhibition was calculated by using the following formula:

% Inhibition = 100 − ((mean of O.D. of test compound − mean of

O.D. of negative control)/(mean of O.D. of positive control − mean of O.D. of negative control) * 100).

The results (% inhibition) were processed by using Soft-Max Pro-Software (Molecular Devices, USA).

3.3. Molecular docking studies protocol

Molecular docking studies were carried out for significant to potent inhibitors **8**, **11–14**, **17**, **18**, **20–22**, and **24**. Since the kinetic analysis showed their non-competitive mode of inhibition, the compounds were docked into the allosteric site of enzyme found by site map analysis module of Maestro 11, Schrodinger [29].

Structures of the compounds were pre-processed through *Ligprep* module from the drug discovery suit of Maestro 11 Schrodinger [30]. Pre-processing generates the correct protonation and possible ionization states. The three-dimensional crystallographic structure of jack bean urease (PDB ID: 4H9M) at 1.52 Å resolution was retrieved from Protein data bank (PDB) RCSB. *Protein Preparation Wizard* [31,32] was used to prepare protein by employing OPLS-3 force field [33]. Missing hydrogens, and partial charges were added to the protein. Followed by restrained minimization to optimize heavy atoms and hydrogens. For docking, a grid box of 10 Å × 10 Å × 10 Å dimension was generated to confine the mass centre of each docked ligand. Rigid receptor docking protocol was run in extra precision (XP) mode of glide [34] using OPLS-3 force field.

3.4. General procedure for the synthesis of compounds 1–25

Tryptamine 0.160 g (1 mmol) was dissolved in dichloromethane, catalytic amount of *tri*methylamine (Et_3N) was added into the reaction mixture, then isocyanates or isothiocayanates (1 mmol) were added, and mixture was kept on stirring for 2–24 h. Reaction progress was monitored with TLC, after the formation of precipitates. It was filtered and washed with hexane to afford final products. The structural determination was carried out mainly by ^{1}H-, and ^{13}C NMR, and mass spectroscopy.

3.5. Spectral data for the synthesized compounds

3.5.1. 1-(2-(1H-Indol-3-yl)ethyl)-3-(naphthalen-1-yl)urea (1)

% Yield: 46, M. p.: 195–197 °C, ^{1}H NMR (300 MHz, DMSO-d_6): δ 10.85 (s, 1H, NH), 8.52 (s, 1H, NH), 8.05 (m, 2H, NH, H-8′), 7.89 (m, 1H, H-5′), 7.59 (m, 2H, H-4′, H-4), 7.55 (m, 2H, H-6′, H-7′), 7.43 (m, 2H, H-2′, H-7), 7.20 (s, 1H, H-2), 7.09 (t, 1H, $J_{5,6/5,4}$ = 7.2 Hz, H-5), 6.99 (t, 1H, $J_{6,5/6,7}$ = 7.3 Hz, H-6), 6.61 (t, 1H, $J_{3',4'/3',2'}$ = 5.3 Hz, H-3′), 3.49 (m, 2H, CH_2), 2.91 (t, $J_{2'',1''}$ = 6.9 Hz, 2H, CH_2), EI-MS *m/z* (% rel. abund.): 329 (M^+, 9), 168 (46), 143 (100).

3.5.2. 1-(2-(1H-Indol-3-yl)ethyl)-3-(4-nitrophenyl)urea (2)

% Yield: 32, M. p.: 178–180 °C, ^{1}H NMR (300 MHz, DMSO-d_6): δ 10.73 (s, 1H, NH), 8.20 (d, 2H, $J_{3',4'/5',6'}$ = 9.3 Hz, H-3′, H-5′), 7.76 (d, 2H, $J_{2',3'/6',5'}$ = 9.3 Hz, H-2′, H-6′), 7.51 (d, 1H, $J_{4,5}$ = 7.5 Hz, H-4), 7.33 (d, 1H, $J_{7,6}$ = 8.1 Hz, H-7), 7.11 (s, 1H, H-2), 7.06 (t, 1H, $J_{5,6/5,4}$ = 7.0 Hz, H-5), 6.97 (t, 1H, $J_{6,5/6,7}$ = 7.0 Hz, H-6), 2.82 (m, 4H, CH_2), EI-MS *m/z* (% rel. abund.): 324 (M^+, 5), 160 (21), 130 (100).

3.5.3. 1-(2-(1H-Indol-3-yl)ethyl)-3-(3-chlorophenyl)urea (3)

% Yield: 42, M. p.: 145–146 °C, ^{1}H NMR (300 MHz, DMSO-d_6): δ 10.83 (s, 1H, NH), 8.71 (s, 1H, NH), 7.67 (s, 1H, NH), 7.63 (d, 1H, $J_{4,5}$ = 7.8 Hz, H-4), 7.34 (d, 1H, $J_{7,6}$ = 7.8 Hz, H-7), 7.24 (m, 3H, H-2′, H-6′, H-4′), 7.08 (t, 1H, $J_{5,6/5,4}$ = 7.5 Hz, H-5), 6.99 (m, 2H, H-6, H-2), 6.23 (t, 1H, $J_{5',\ 6'/5',4'}$ = 5.2 Hz, H-5′), 3.75 (m, 2H, CH_2), 2.86 (t, 2H, $J_{2'',1''}$ = 7.2 Hz, CH_2), EI-MS *m/z* (% rel. abund.): 313 (M^+, 6), 315 (M^+ + 2, 2), 155 (30), 130 (100), HREI-MS *m/z*: calcd for $C_{17}H_{16}NO_3Cl$ [313.0991], found [313.0982].

3.5.4. 1-(2-(1H-Indol-3-yl)ethyl)-3-(2-(trifluoromethyl)phenyl)urea (4)

% Yield: 22, M. p.: 128–130 °C, ^{1}H NMR (400 MHz, CD_3OD): δ 7.78 (d, 1H, $J_{3',4'}$ = 8.4 Hz, H-3′), 7.60 (t, 2H, $J_{4',3'/5',4'}$ = 8.4 Hz, H-4′, H-5′), 7.53 (d, 1H, $J_{4,5}$ = 7.6 Hz, H-4), 7.33 (d, 1H, $J_{7,6}$ = 8.0 Hz, H-7), 7.21 (t, 1H, $J_{5,4/5,6}$ = 7.6 Hz, H-5), 7.08 (m, 2H, H-2, H-6′), 7.07 (t, 1H, $J_{6,5/6,7}$ = 7.2 Hz, H-6), 3.51 (t, 2H, $J_{1'',2''}$ = 7.2 Hz, CH_2), 2.97 (t, 2H, $J_{2'',1''}$ = 6.8 Hz, CH_2), EI-MS *m/z* (% rel. abund.): 347 (M^+, 2), 149 (24), 143 (100), HREI-MS *m/z* : calcd for $C_{18}H_{16}ON_3F_3$ [347.1240], found [347.1234].

3.5.5. 1-(2-(1H-Indol-3-yl)ethyl)-3-(3-(trifluoromethyl)phenyl)urea (5)

% Yield: 29, M. p.: 155–157 °C, ^{1}H NMR (400 MHz, DMSO-d_6): δ 10.81 (s, 1H, NH), 8.89 (s, 1H, NH), 8.02 (s, 1H, NH), 7.56 (d, 1H, $J_{4,5}$ = 5.7 Hz, H-4), 7.44 (m, 2H, H-2′, H-4′), 7.34 (d, 1H, $J_{7,6}$ = 6.0 Hz, H-7), 7.20 (m, 2H, H-2, H-6′), 7.07 (t, 1H, $J_{5,6/5,4}$ = 5.4 Hz, H-5), 6.98 (t, 1H, $J_{6,5/6,7}$ = 5.4 Hz, H-6), 6.29 (t, 1H, $J_{5',6'/5',4'}$ = 4.2 Hz, H-5′), 3.42 (m, 2H, CH_2), 2.87 (t, 2H, $J_{2'',1''}$ = 5.4 Hz, CH_2), EI-MS *m/z* (% rel. abund.): 347 (M^+, 7), 143 (46), 130 (100), HREI-MS *m/z* : calcd for $C_{18}H_{16}ON_3F_3$ [347.1235], found [347.1245].

3.5.6. 1-(2-(1H-Indol-3-yl)ethyl)-3-phenylthiourea (6)

% Yield: 50, M. p.: 188–190 °C, ^{1}H NMR (300 MHz, DMSO-d_6): δ 10.82 (s, 1H, NH), 9.52 (s, 1H, NH), 7.71 (br.s, 1H, NH), 7.63 (d, 1H, $J_{4,5}$ = 7.8 Hz, H-4), 7.34 (m, 5H, H-7, H-2′, H-3′, H-5′, H-6′), 7.16 (s, 1H, H-2), 7.10 (m, 2H, H-4′, H-5), 6.99 (t, 1H, $J_{6,5/6,7}$ = 7.0 Hz, H-6), 3.75 (d, 2H, $J_{1'',2''}$ = 5.7 Hz, CH_2), 2.99 (t, 2H, $J_{2'',1''}$ = 7.2 Hz, CH_2), EI-MS *m/z* (% rel. abund.): 295 (M^+, 3), 135 (34), 130 (100).

3.5.7. 1-(2-(1H-Indol-3-yl)ethyl)-3-(4-nitrophenyl)thiourea (7)

Yield: 46%, M. p.: 197–199 °C, ^{1}H NMR (400 MHz, DMSO-d_6): δ 10.85 (s, 1H, NH), 10.21 (s, 1H, NH), 8.28 (br.s, 1H, NH), 8.14 (d, 2H, $J_{3',4'/5',6'}$ = 6.9 Hz, H-3′, H-5′), 7.57 (d, 2H, $J_{2',3'/6',5'}$ = 6.9 Hz, H-2′, H-6′), 7.63 (d, 1H, $J_{4,5}$ = 5.7 Hz, H-4), 7.35 (d, 1H, $J_{7,6}$ = 6.0 Hz, H-7), 7.20 (s, 1H, H-2), 7.08 (t, 1H, $J_{5,6/5,4}$ = 5.7 Hz, H-5), 6.99 (t, 1H, $J_{6,5/6,7}$ = 5.4 Hz, H-6), 3.80 (br.s, 2H, CH_2), 3.02 (t, 2H, $J_{2'',1''}$ = 5.4 Hz, CH_2), ^{13}C NMR (600 MHz, DMSO-d_6): δ179.8, 146.3, 141.7, 136.3, 127.2, 124.6, 122.9, 121.0, 120.3, 118.4, 118.3, 111.4, 111.3, 44.6, 24.1, EI-MS *m/z* (% rel. abund.): 340 (M^+, 13), 150 (56), 130 (100), HREI-MS *m/z*: Calcd for $C_{17}H_{16}N_4O_2S$ [340.0992], found [340.0994].

3.5.8. 1-(2-(1H-Indol-3-yl)ethyl)-3-(3-fluorophenyl)thiourea (8)

% Yield: 45, M. p.: 124–127 °C, ^{1}H NMR (400 MHz, DMSO-d_6): δ 10.82 (s, 1H, NH), 9.68 (s, 1H, NH), 7.89 (br.s, 1H, NH), 7.63 (d, 1H, $J_{4,5}$ = 5.7 Hz, H-4), 7.49 (d, 1H, $J_{6',5'}$ = 8.7 Hz, H-6′), 7.34 (d, 1H, $J_{7,6}$ = 6.3 Hz, H-7), 7.30 (m, 1H, H-5′), 7.17 (s, 1H, H-2), 7.11 (m, 2H, H-2′, H-4′), 6.99 (t, 1H, $J_{5,6/5,4}$ = 5.7 Hz, H-5), 6.99 (m, 1H, H-6), 3.77 (t, 2H, $J_{1'',2''}$ = 7.2 Hz, CH_2), 2.99 (t, 2H, $J_{2'',1''}$ = 7.2 Hz, CH_2), EI-MS *m/z* (% rel. abund.): 313 (M^+, 6), 153 (16), 143 (100).

3.5.9. 1-(2-(1H-Indol-3-yl)ethyl)-3-(5-chloro-2-methylphenyl)thiourea (9)

% Yield: 34, M. p.: 136–139 °C, ^{1}H NMR (400 MHz, DMSO-d_6): δ 10.80 (s, 1H, NH), 9.09 (s, 1H, NH), 7.69 (br.s, 1H, NH), 7.62 (d, 1H, $J_{4,5}$ = 5.7 Hz, H-4), 7.35 (s, 1H, H-2′), 7.33 (d, 1H, $J_{7,6}$ = 6.3 Hz, H-7), 7.25 (d, 1H, $J_{5',4'}$ = 6.0 Hz, H-5′), 7.19 (dd, 1H, $J_{4',5'}$ = 4.5 Hz, $J_{4',6'}$ = 1.5 Hz, H-4′), 7.14 (s, 1H, H-2), 7.07 (t, 1H, $J_{5,6/5,4}$ = 5.5 Hz, H-5), 6.98 (t, 1H, $J_{6,5/6,7}$ = 5.5 Hz, H-6), 3.72 (br.s, 2H, CH_2), 2.97 (t, 2H, $J_{2'',1''}$ = 5.4 Hz, CH_2), EI-MS *m/z* (% rel. abund.): 343 (M^+, 4), 345 (M^+ + 2, 2), 130 (100), HREI-MS *m/z*: calcd for $C_{18}H_{18}N_3ClS$ [343.0906], found [343.0910].

3.5.10. 1-(2-(1H-Indol-3-yl)ethyl)-3-(2-bromophenyl)thiourea (10)

Yield: 54%, M. p.: 142–144 °C, ^{1}H NMR (400 MHz, DMSO-d_6): δ 10.81 (s, 1H, NH), 9.09 (s, 1H, NH), 7.90 (br.s, 1H, NH), 7.60 (m, 2H, H-4, H-5′), 7.56 (d, 1H, $J_{3',4'}$ = 5.4 Hz, H-3′), 7.35 (m, 2H, H-7, H-3′), 7.16 (m, 2H, H-2, H-4), 7.07 (t, 1H, $J_{5,6/5,4}$ = 5.5 Hz, H-5), 6.99 (t, 1H,

$J_{6,5/6,7}$ = 5.5 Hz, H-6), 3.72 (br.s, 2H, CH_2), 2.97 (t, 2H, $J_{2'',1''}$ = 5.4 Hz, CH_2), ^{13}C NMR (300 MHz, DMSO-d_6): δ181.1, 137.4, 136.2, 132.6, 129.7, 127.7, 127.5, 127.2122.8, 120.9, 120.3, 118.5, 118.2, 111.5, 111.3, 44.8, 24.6, EI MS *m/z* (% rel. abund.): 373 (M^+, 0.5), 375 (M^+ + 2, 0.5), 130 (100), HREI-MS *m/z*: Calcd for $C_{17}H_{16}N_3BrS$ [373.0285], found [373.0284].

*3.5.11. 1-(2-(1H-Indol-3-yl)ethyl)-3-(2-fluorophenyl)thiourea (**11**)*

% Yield: 44, M. p.: 137–139 °C, ^{1}H NMR (400 MHz, DMSO-d_6): δ 10.82 (s, 1H, NH), 9.23 (s, 1H, NH), 7.89 (s, 1H, NH), 7.66 (m, 2H, H-4, H-6′), 7.34 (d, 1H, $J_{7,6}$ = 6.0 Hz, H-7), 7.23 (m, 2H, H-3′, H-5′), 7.15 (m, 2H, H-2, H-4′), 7.07 (t, 1H, $J_{5,6/5,7}$ = 5.5 Hz, H-5), 6.99 (t, 1H, $J_{6,5/6,7}$ = 5.5 Hz, 1H, H-6), 3.37 (br.s, 2H, CH_2), 2.97 (t, 2H, $J_{2'',1''}$ = 5.4 Hz, CH_2), EI-MS *m/z* (% rel. abund.): 313 (M^+, 1), 152 (19), 130 (100), HREI-MS *m/z*: calcd for $C_{17}H_{16}N_3FS$ [313.1034], found [313.1049].

*3.5.12. 1-(2-(1H-Indol-3-yl)ethyl)-3-(2,6-dimethylphenyl)thiourea (**12**)*

% Yield: 39, M. p.: 184–186 °C, ^{1}H NMR (400 MHz, DMSO-d_6): δ 10.77 (s, 1H, NH), 9.06 (s, 1H, NH), 7.63 (d, 1H, $J_{4,5}$ = 6.0 Hz, H-4), 7.32 (d, 1H, $J_{7,6}$ = 6.3 Hz, H-7), 7.07 (m, 5H, H-3′, H-4′, H-5′, H-2, H-5), 6.97 (t, 1H, $J_{6,5/6,7}$ = 5.4 Hz, H-6), 3.67 (s, 2H, CH_2), 2.90 (s, 2H, CH_2), 2.48 (s, 6H, CH_3), EI-MS *m/z* (% rel. abund.): 323 (M^+, 22), 181 (41), 143 (100), HREI-MS *m/z*: calcd for $C_{19}H_{21}N_3S$ [323.1434], found [323.1456].

*3.5.13. 1-(2-(1H-Indol-3-yl)ethyl)-3-(3-bromophenyl)thiourea (**13**)*

Yield: 56%, M. p.: 114–117 °C, ^{1}H NMR (400 MHz, DMSO-d_6): δ 10.83 (s, 1H, NH), 9.65 (s, 1H, NH), 7.91 (s, 1H, NH), 7.78 (s, 1H, H-6′), 7.63 (d, 1H, $J_{4,5}$ = 5.7 Hz, H-4), 7.35 (d, 1H, $J_{7,6}$ = 6.3 Hz, H-7), 7.29 (m, 3H, H-3′, H-4′, H-5′), 7.17 (s, 1H, H-2), 7.08 (t, 1H, $J_{5,6/5,4}$ = 5.5 Hz, H-5), 6.99 (t, 1H, $J_{6,5/6,7}$ = 5.4 Hz, H-6), 3.76 (br.s, 2H, CH_2), 2.99 (t, 2H, $J_{2'',1''}$ = 5.7 Hz, CH_2), ^{13}C NMR (300 MHz, DMSO-d_6): δ180.0, 141.0, 136.2, 130.3, 127.1, 126.2, 124.7, 122.7, 121.2, 121.0, 120.9, 118.4, 118.1, 111.4, 111.3, EI MS *m/z* (% rel. abund.): 373 (M^+, 2), 375 (M^+ + 2, 2), 130 (100), HREI-MS *m/z*: Calcd for $C_{17}H_{16}N_3BrS$ [373.0219], found [373.0248].

*3.5.14. 1-(2-(1H-Indol-3-yl)ethyl)-3-(o-tolyl)thiourea (**14**)*

Yield: 62%, M. p.: 185–187 °C, ^{1}H NMR (400 MHz, DMSO-d_6): δ 10.79 (s, 1H, NH), 9.07 (s, 1H, NH), 7.63 (d, 1H, $J_{4,5}$ = 5.7 Hz, H-4), 7.33 (d, 1H, $J_{7,6}$ = 6.0 Hz, H-7), 7.21 (m, 4H, H-2′, H-6′, H-3′, H-5′), 7.11 (s, 1H, H-2), 7.07 (t, 1H, $J_{5,6/5,4}$ = 5.7 Hz, H-5), 6.98 (t, 1H, $J_{6,5/6,7}$ = 5.5 Hz, H-6), 3.71 (br.s, 2H, CH_2), 2.95 (t, 2H, $J_{2'',1''}$ = 5.4 Hz, CH_2), 2.14 (s, 3H, OCH_3), ^{13}C NMR (300 MHz, DMSO-d_6): δ180.8, 136.2, 130.5, 127.7, 127.2, 126.5, 126.3, 122.7, 120.9, 118.5, 118.2, 111.6, 111.3, 44.8, 24.7, 17.6, EI MS *m/z* (% rel. abund.): 309 (M^+, 21), 167 (35), 143 (1 0 0), HREI-MS *m/z*: Calcd for $C_{18}H_{19}N_3S$ [309.1286], found [309.1300].

*3.5.15. 1-(2-(1H-Indol-3-yl)ethyl)-3-(2,5-dichlorophenyl)thiourea (**15**)*

% Yield: 54, M. p.: 160–162 °C, 1H NMR (400 MHz, DMSO-d_6): δ 10.83 (s, 1H, NH), 9.23 (s, 1H, NH), 8.21 (s, 1H, NH), 7.90 (s, 1H, H-6′), 7.62 (d, 1H, J4′,3′ = 6.0 Hz, H-4′), 7.51 (d, 1H, J4,5 = 6.3 Hz, H-4), 7.34 (d, 1H, J7,6 = 6.0 Hz, H-7), 7.26 (d, 1H, J3′,4′ = 6.3 Hz, H-3′), 7.17 (s, 1H, H-2), 7.06 (t, 1H, J5,6/5,4 = 5.4 Hz, H-5), 6.97 (t, 1H, J 6,5/6,7 = 5.4 Hz, H-6), 3.76 (br.s, 2H, CH2), 2.99 (t, 2H, J2″,1″ = 5.4 Hz, CH2), FAB-MS + ve *m/z* (% rel. abund.): 364 (M +).

*3.5.16. 1-(2-(1H-Indol-3-yl)ethyl)-3-(4-chlorophenyl)thiourea (**16**)*

% Yield: 47, M. p.: 119–121 °C, ^{1}H NMR (400 MHz, DMSO-d_6): δ 10.83 (s, 1H, NH), 8.61 (s, 1H, NH), 7.83 (s, 1H, NH), 7.63 (d, 1H, $J_{4,5}$ = 5.7 Hz, H-4), 7.40 (d, 2H, $J_{3',4'/5',6'}$ = 6.6 Hz, H-3′, H-5′), 7.34 (m, 3H, H-2′, H-6′, H-7), 7.17 (s, 1H, H-2), 7.08 (t, 1H, $J_{5,6/5,4}$ = 5.7 Hz, H-5), 6.97 (t, 1H, $J_{6,5/6,7}$ = 5.5 Hz, H-6), 3.75 (br.s, 2H, CH_2), 2.98 (t, 2H, $J_{2'',1''}$ = 5.4 Hz, CH_2), EI-MS *m/z* (% rel. abund.): 329 (M^+, 4), 331 (M^+ + 2, 1), 171 (53), 130 (100), 127 (64), HREI-MS *m/z*: calcd for $C_{17}H_{16}N_3SCl$ [329.0732], found [329.0753].

*3.5.17. 1-(2-(1H-Indol-3-yl)ethyl)-3-(2,4-dimethoxyphenyl)thiourea (**17**)*

% Yield: 42, M. p.: 126–128 °C, ^{1}H NMR (400 MHz, DMSO-d_6): δ 10.80 (s, 1H, NH), 8.74 (s, 1H, NH), 7.62 (d, 1H, $J_{4,5}$ = 5.7 Hz, H-4), 7.41 (br. s, 1H, NH), 7.33 (m, 2H, H-7, H-6′), 7.11 (s, 1H, H-2), 7.06 (t, 1H, $J_{5,6/5,4}$ = 5.4 Hz, H-5), 6.97 (t, 1H, $J_{6,5/6,7}$ = 5.5 Hz, H-6), 6.58 (d, 1H, $J_{3',5'}$ = 2.1 Hz, 1H, H-3′), 6.48 (dd, 1H, $J_{5',6'}$ = 4.5 Hz, $J_{5',3'}$ = 2.1 Hz, H-5′), 3.75 (m, 8H, CH_2, OCH_3, OCH_3), 2.92 (t, 2H, $J_{2'',1''}$ = 5.4 Hz, CH_2), EI-MS *m/z* (% rel. abund.): 355 (M^+, 1.1), 357 (M^{+2}, 0.3), 290 (48), 144 (100), HREI-MS *m/z*: calcd for $C_{19}H_{21}O_2N_3S$ [355.1338], found [355.1354].

*3.5.18. 1-(2-(1H-Indol-3-yl)ethyl)-3-(2-methoxyphenyl)thiourea (**18**)*

% Yield: 38, M. p.: 116–118 °C, ^{1}H NMR (400 MHz, DMSO-d_6): δ 10.82 (s, 1H, NH), 8.90 (s, 1H, NH), 7.85 (s, 1H. NH), 7.77 (d, 1H, $J_{3',4'}$ = 5.4 Hz, H-3′), 7.63 (d, 1H, $J_{4,5}$ = 5.7 Hz, H-4), 7.34 (d, 1H, $J_{7,6}$ = 6.0 Hz, H-7), 7.14 (m, 5H, H-5′, H-6′, H-4′, H-5, H-2), 6.90 (t, 1H, $J_{6,5/6,7}$ = 5.7 Hz, H-6), 3.77 (m, 5H, CH_2, OCH_3), 2.96 (t, 2H, $J_{2'',1''}$ = 5.7 Hz, CH_2), EI-MS *m/z* (% rel. abund.): 325 (M^+, 1), 144 (55), 130 (100), HREI-MS *m/z*: calcd for $C_{18}H_{19}N_3SO$ [325.1227], found [325.1249].

*3.5.19. 1-(2-(1H-Indol-3-yl)ethyl)-3-(2-chlorophenyl)thiourea (**19**)*

% Yield: 45, M. p.: 143–146 °C, ^{1}H NMR (400 MHz, DMSO-d_6): δ 10.83 (s, 1H, NH), 9.16 (s, 1H, NH), 7.95 (s, 1H, NH), 7.63 (d, 2H, $J_{4,5/3',4'}$ = 5.7 Hz, H-4, H-3′), 7.48 (d, 1H, $J_{7,6}$ = 5.7 Hz, H-7), 7.34 (m, 2H, H-5′, H-6′), 7.22 (t, 1H, $J_{4',5'/4',3'}$ = 5.7 Hz, H-4′), 7.16 (s, 1H, H-2), 7.07 (t, 1H, $J_{5,6/5,7}$ = 5.5 Hz, H-5), 6.99 (t, 1H, $J_{6,5/6,7}$ = 5.5 Hz, H-6), 3.75 (s, 2H, CH_2), 2.98 (t, 2H, $J_{2'',1''}$ = 5.4 Hz, CH_2), EI-MS *m/z* (% rel. abund.): 329 (M^+, 2), 331 (M^+ + 2, 0.3), 169 (64), 130 (100), HREI-MS *m/z*: calcd for $C_{17}H_{16}N_3SCl$ [329.0742], found [329.0753].

*3.5.20. 1-(2-(1H-Indol-3-yl)ethyl)-3-(2,4-difluorophenyl)thiourea (**20**)*

% Yield: 51, M. p.: 165–167 °C, ^{1}H NMR (400 MHz, CD_3OD): δ 7.62 (d, 1H, $J_{4,5}$ = 6.0 Hz, H-4), 7.33 (d, 1H, $J_{7,6}$ = 6.0 Hz, H-7), 7.09 (m, 2H, H-6′, H-3′), 6.97 (m, 2H, H-2, H-5), 6.95 (t, 1H, $J_{6,5/6,7}$ = 6.1 Hz, H-6), 3.85 (br.s, 2H, CH_2), 3.07 (t, 2H, $J_{2'',1''}$ = 5.4 Hz, CH_2), EI-MS *m/z* (% rel. abund.): 331 (M^+, 8), 143 (100), 130 (86), HREI-MS *m/z*: calcd for $C_{17}H_{15}N_3SF_2$ [331.0946], found [331.0955].

*3.5.21. 1-(2-(1H-Indol-3-yl)ethyl)-3-(3-methoxyphenyl)thiourea (**21**)*

% Yield: 47, M. p.: 163–165 °C, ^{1}H NMR (400 MHz, CD_3OD): δ 7.63 (d, 1H, $J_{4,5}$ = 6.0 Hz, H-4), 7.33 (d, 1H, $J_{7,6}$ = 6.0 Hz, H-7), 7.15 (m, 3H, H-5, H-2, H-5′), 7.00 (t, 1H, $J_{6,5/6,7}$ = 5.5 Hz, H-6), 6.75 (s, 1H, H-2′), 6.71 (d, 1H, $J_{6',5'}$ = 6.3 Hz, H-6′), 6.62 (d, 1H, $J_{4',5'}$ = 6.0 Hz, H-4′), 3.87 (t, 2H, $J_{1'',2''}$ = 4.5 Hz, CH_2), 3.65 (s, 3H, OCH_3), 3.08 (t, 2H, $J_{2'',1''}$ = 5.1 Hz, CH_2), EI-MS *m/z* (% rel. abund.): 325 (M^+, 13), 143 (100), 130 (92), HREI-MS *m/z*: calcd for $C_{18}H_{19}N_3SO$ [325.1275], found [325.1249].

*3.5.22. 1-(2-(1H-Indol-3-yl)ethyl)-3-(3,5-dimethylphenyl)thiourea (**22**)*

% Yield: 45, M. p.: 122–124 °C, ^{1}H NMR (400 MHz, CD_3OD): δ 7.62 (d, 1H, $J_{4,5}$ = 6.0 Hz, H-4), 7.33 (d, 1H, $J_{7,6}$ = 6.0 Hz, H-7), 7.09 (m, 2H, H-5, H-2), 7.00 (t, 1H, $J_{6,5/6,7}$ = 5.7 Hz, H-6), 6.78 (s, 1H, H-4′), 6.61 (s, 2H, H-2′, H-6′), 3.88 (t, 2H, $J_{1'',2''}$ = 4.8 Hz, CH_2), 3.07 (t, 2H, $J_{2'',1''}$ = 5.1 Hz, CH_2), 2.15 (s, 6H, CH_3), EI-MS *m/z* (% rel. abund.): 323 (M^+, 13), 163 (45), 143 (100), 130 (85), HREI-MS *m/z*: calcd for $C_{19}H_{21}N_3S$ [323.1452], found [323.1456].

*3.5.23. 1-(2-(1H-Indol-3-yl)ethyl)-3-(2,3-dichlorophenyl)thiourea (**23**)*

% Yield: 35, M. p.: 166–168 °C, ^{1}H NMR (400 MHz, CD_3OD): δ 7.63 (d, 1H, $J_{4,5}$ = 6.0 Hz, H-4), 7.41 (m, 2H, H-4′, H-5′), 7.33 (d, 1H, $J_{7,6}$ = 6.0 Hz, H-7), 7.10 (t, 1H, $J_{5,6/5,4}$ = 6.1 Hz, H-5), 7.09 (m, 2H, H-2, H-6′), 7.01 (t, 1H, $J_{6,5/6,7}$ = 5.5 Hz, H-6), 3.86 (s, 2H, CH_2), 3.08 (t, 1H, $J_{2'',1''}$ = 5.4 Hz, CH_2), FAB-MS + ve *m/z* (% rel. abund.): 364 (M^+),

HREI-MS *m/z*: calcd for $C_{17}H_{15}N_3SCl_2$ [363.0365], found [363.0364].

*3.5.24. 1-(2-(1H-Indol-3-yl)ethyl)-3-(4-methoxyphenyl)thiourea (**24**)*

% Yield: 54, M. p.: 163–166 °C, ^{1}H NMR (400 MHz, CD_3OD): δ 7.61 (d, 1H, $J_{4,5}$ = 8.0 Hz, H-4), 7.33 (d, 1H, $J_{7,6}$ = 6.0 Hz, H-7), 7.10 (t, 1H, $J_{5,6/5,4}$ = 6.8 Hz, H-5), 7.02 (s, 1H, H-2), 6.98 (t, 1H, $J_{6,7/6,5}$ = 7.4 Hz, H-6), 6.93 (d, 2H, $J_{3',2'/5',6'}$ = 8.8 Hz, H-3′, H-5′), 6.79 (d, 2H, $J_{2',3'/6',5'}$ = 8.4 Hz, H-2′, H-6′), 3.83 (t, 2H, $J_{1'',2''}$ = 6.4 Hz, CH_2), 3.75 (s, 1H, OCH_3, H-4′), 3.03 (t, 2H, $J_{2'',1''}$ = 6.8 Hz, CH_2), 2.15 (s, 6H, CH_3), EI-MS *m/z* (% rel. abund.): 325 (M^+, 13), 165 (45), 143 (100), 130 (85), HREI-MS *m/z*: calcd for $C_{18}H_{19}N_3SO$ [325.1228], found [325.1249].

*3.5.25. 1-(2-(1H-Indol-3-yl)ethyl)-3-(4-bromophenyl)thiourea (**25**)*

% Yield: 44, M. p.: 129–131 °C, ^{1}H NMR (400 MHz, CD_3OD): δ 7.62 (d, 1H, $J_{4,5}$ = 6.0 Hz, H-4), 7.35 (m, 3H, H-7, H-3′, H-5′), 7.11 (m, 4H, H-5, H-2, H-2′, H-6′), 7.01 (t, 1H, $J_{6,5/6,7}$ = 5.5 Hz, H-6), 3.86 (s, 2H, CH_2), 3.08 (t, 2H, $J_{2'',1''}$ = 5.4 Hz, CH_2), EI-MS *m/z* (% rel. abund.): 372 (M^+ 1), 374 (M^+ + 2, 1), 130 (100), HREI-MS *m/z*: calcd for $C_{17}H_{16}N_3SBr$ [373.0221], found [373.0248].

4. Conclusion

Twenty five derivatives of tryptamine **1–25** were synthesized, and evaluated for their urease inhibitory activity. Nine of them **11–17**, **22**, and **24** were found to be active with IC_{50} values between 11.4 ± 0.4–19.7 ± 0.83 μM, five compounds **8**, **10**, **18**, **19**, and **21** with IC_{50} of 21.3 ± 1.5–27.1 ± 0.64 μM showed activity comparable to standard thiourea, while others were inactive against urease. Moreover, only thiourea analogues showed a better inhibitory activity. All the synthetic derivatives were non-cytotoxic. Kinetic studies showed that most of the active compounds exhibit non-competitive type of inhibition, however, compounds **8** and **13** showed mixed-type of inhibition. The ligand-enzyme binding modes, and interactions were predicted using molecular docking studies. These results identified several lead molecules for further studies.

Acknowledgement

This work was supported by the Higher Education Commission (HEC), Pakistan (Project No. 20-1910), under the National Research Program for Universities.

References

[1] T. Tanzila Arshad, K.M. Khan, N. Rasool, U. Salar, S. Hussain, H. Asghar, M. Ashraf, A. Wadood, M. Riaz, S. Perveen, M. Taha, N.H. Ismail, 5-Bromo-2-aryl benzimidazole derivatives as non-cytotoxic potential dual inhibitors of α-glucosidase and urease enzymes, Bioorg. Chem. 72 (2017) 21–31.
[2] J. Ruckriemen, O. Klemm, T. Henle, Manuka honey (*Leptospermum scoparium*) inhibits jack bean urease activity due to methylglyoxal and dihydroxyacetone, Food Chem. 230 (2017) 540–546.
[3] L.V. Modolo, A.X. De Souza, L.P. Horta, P.D. Araujo, A. Fatima, An overview on the potential of natural products as ureases inhibitors: a review, J. Adv. Res. 6 (2015) 35–44.
[4] J.L. Boer, S.B. Mulrooney, R.P. Hausinger, Nickel-dependent metalloenzymes, Arch. Biochem. Biophys. 544 (2014) 142–152.
[5] L. Pan, C. Wang, K. Yan, K. Zhao, G. Sheng, H. Zhu, X. Zhao, Z. Qu, F. Niu, Z. You, Synthesis, structures and *Helicobacter pylori* urease inhibitory activity of copper (II) complexes with *tri*dentate aroylhydrazone ligands, J. Inorg. Biochem. 159 (2016) 22–28.
[6] M.J. Maroney, S. Ciurli, Non redox nickel enzymes, Chem. Rev. 114 (2014) 4206–4228.
[7] W. Lin, V. Mathys, E.L. Yin Ang, V.H. Qi Koh, M.M. Gomez, M.L.T. Ang, S.T. Zainul Rahim, M.P. Tan, K. Pethe, S. Alonsoa, Urease activity represents an alternative pathway for *Mycobacterium tuberculosis* nitrogen metabolism, Infect. Immun. 80 (8) (2012) 2771–2779.
[8] G.M. Young, D. Amid, V.L. Miller, A bifunctional urease enhances survival of pathogenic *Yersinia enterocolitica* and *Morganella morganii* at low pH, J. Bacteriol. 178 (22) (1996) 6487–6495.
[9] G.M. Cox, J. Mukherjee, G.L. Cole, A. Casadevall, J.R. Perfect, Urease as a virulence factor in experimental *Cryptococcosis*, Infect. Immun. 68 (2) (2000) 443–448.
[10] K.M. Khan, F. Naz, M. Taha, A. Khan, S. Perveen, M.I. Choudhary, W. Voelter, Synthesis and in vitro urease inhibitory activity of *N*, *N*″-disubstituted thioureas, Eur. J. Med. Chem. 74 (2014) 314–323.
[11] M. Amin, F. Anwar, F. Naz, T. Mehmood, N. Saari, Anti-*Helicobacter pylori* and urease inhibition activities of some traditional medicinal plants, Molecules 18 (2013) 2135–2149.
[12] L.T.B. Upadhyay, Urease inhibitors: a review, Indian J. Biotechnol. 11 (2012) 381–388.
[13] M.I. Mustafa, M.A. Hapipah, M.A. Abdulla, R.T. Ward, Synthesis, structural characterization, and antiulcerogenic activity of Schiff base ligands derived from tryptamine and 5-chloro, 5-nitro, 3,5-ditertiarybutylsalicylaldehyde and their nickel(II), copper(II), and zinc(II) complexes, Polyhedron 28 (2009) 3993–3998.
[14] S.J. Qu, G.F. Wang, W.H. Duan, S.Y. Yao, J.P. Zuo, C.H. Tan, Tryptamine derivatives as novel non nucleosidic inhibitors against hepatitis B virus, Bioorg. Med. Chem. 19 (2011) 3120–3127.
[15] M.S. Estevao, L.C. Carvalho, D. Ribeiro, D. Couto, M. Freitas, A. Gomes, L.M. Ferreira, E. Fernandes, M. Manuel, B. Marques, Antioxidant activity of unexplored indole derivatives: Synthesis and screening, Eur. J. Med. Chem. 45 (2010) 4869–4878.
[16] S. Perveen, S. Mustafa, K. Qamar, A. Dar, K.M. Khan, M.I. Choudhary, A. Khan, W. Voelter, Antiproliferative effects of novel urea derivatives against human prostate and lung cancer cells; and their inhibition of β-glucuronidase activity, Med. Chem. Res. 23 (2014) 1099–1113.
[17] A.U. Rehman, M. Ayoub, M.A. Abbasi, S. Gul, M. Ashraf, R. Hassan, I. Ahmad, K.M. Khan, Synthesis of *N*-substituted derivatives of *N*-(4-(*N*-(5-choloro-2 methoxyphenyl)sulfamoyl)phenyl)acetamide with potential antiurease activity, J. Chem. Soc. Pakistan 35 (2013) 1516–1521.
[18] S.A. Shahzad, M. Yar, Z.A. Khan, I.U. Khan, S.A.R. Naqvi, N. Mahmood, K.M. Khan, Microwave-assisted solvent free efficient synthesis of 1,3,4-oxazole-2(3*H*)-thiones and their *in vitro* Urease Inhibitory Activity, Eur. J. Chem. 3 (2012) 143–146.
[19] T. Akhtar, S. Hameed, K.M. Khan, A. Khan, M.I. Choudhary, Design, synthesis, and urease inhibition studies of some 1,3,4-oxadiazole and 1,2,4-*tri*azoles derived from mandelic acid, J. Enzyme Inhib. Med. Chem. 25 (2010) 572–576.
[20] H. Pervez, N. Manzoor, M. Yaqub, A. Khan, K.M. Khan, F. Nasim, M.I. Choudhary, Synthesis and Urease inhibitory properties of some new *N*-4-substituted 5-Nitroisatin-3-thiosemicarbazones, Lett. Drug Des. Discovery 7 (2010) 102–108.
[21] S. Ceylana, H. Bayrakb, A. Demirbasb, S. Ulkerc, S.A. Karaogluc, N. Demirbasb, Synthesis of some new hybrid molecules containing several azole moieties and investigation of their biological activities, Russ. J. Bioorg. Chem. 40 (2014) 314–329.
[22] L. Novak, M. Hanania, P. Kovacs, P. Kolonits, C. Szantaya, Preparation of novel cyanoguanidine derivatives of tryptamines, Synthesis 1 (2001) 108–118.
[23] T. Bosanac, C.S. Wilcox, A photo-activated precipiton for reagent sequestration in solution-phase synthesis, J. Am. Chem. Soc. 124 (2002) 4194–4195.
[24] W. Zhang, C.H. Chen, T. Nagashima, Fluorous electrophilic scavengers for solution-phase parallel synthesis, Tetrahedron Lett. 44 (2003) 2065–2068.
[25] T. Akhtar, S. Hameed, K.M. Khan, M.I. Choudhary, Syntheses, urease inhibition, and antimicrobial studies of some chiral 3-substituted-4-amino-5-thioxo-1*H*,4 *H*-1,2,4-*tri*azoles, Med. Chem. 4 (2008) 539–543.
[26] K.M. Khan, S. Iqbal, M.A. Lodhi, G.M. Maharvi, Zia-Ullah, M.I. Choudhary, Attaur-Rahman, S. Perveen, Biscoumarin: New class of urease inhibitors, economical synthesis and activity, Bioorg. Med. Chem. 12 (2004) 1963–1968.
[27] M. Taha, N.H. Ismail, S. Imran, M.H. Mohamad, A. Wadood, F. Rahim, S.M. Saad, Ashfaq ur Rehman, K.M. Khan, Synthesis, α-glucosidase inhibitory, cytotoxicity and docking studies of 2-aryl-7-methylbenzimidazoles, Bioorg. Chem. 65 (2016) 100–109.
[28] T. Mosmann, Rapid colorimetric assay for cellular growth and survival: application to proliferation and cytotoxicity assays, J. Immunol. Methods 65 (1983) 55–63.
[29] T.A. Halgren, Identifying and characterizing binding sites and assessing druggability, J. Chem. Inf. Model. 49 (2) (2009) 377–389.
[30] Schrödinger Release 2017-4: LigPrep, Schrödinger, LLC, New York, NY, 2017.
[31] G.M. Sastry, M. Adzhigirey, T. Day, R. Annabhimoju, W. Sherman, Protein and ligand preparation: parameters, protocols, and influence on virtual screening enrichments, J. Comput. Aided Mol. Des. 27 (3) (2013) 221–234.
[32] Schrödinger Release 2017-4: Schrödinger Suite 2017-4 Protein Preparation Wizard; Epik, Schrödinger, LLC, New York, NY, 2016. Impact, Schrödinger, LLC, New York, NY, 2016; Prime, Schrödinger, LLC, New York, NY, 2017.
[33] E. Harder, W. Damm, J. Maple, C. Wu, M. Reboul, J.Y. Xiang, J.W. Kaus, OPLS3: a force field providing broad coverage of drug-like small molecules and proteins, J. Chem. Theory Comput. 12 (1) (2015) 281–296.
[34] R.A. Friesner, R.B. Murphy, M.P. Repasky, L.L. Frye, J.R. Greenwood, T.A. Halgren, D.T. Mainz, Extra precision glide: Docking and scoring incorporating a model of hydrophobic enclosure for protein − ligand complexes, J. Med. Chem. 49 (21) (2006) 6177–6196.